

1 Technical Note: Preventing CO₂ overestimation from mercuric or
2 copper (II) chloride preservation of dissolved greenhouse gases in
3 freshwater samples

4

5 François Clayer^{1*}, Jan Erik Thrane¹, Kuria Ndungu¹, Andrew King¹, Peter Dörsch², Thomas Rohrlack²

6

7 ¹Norwegian Institute for Water Research (NIVA), Økernveien 94, 0579 Oslo, Norway

8

9 ²Faculty of Environmental Sciences and Natural Resource Management, Norwegian University of
10 Life Sciences, PO Box 5003, 1432 Ås, Norway

11

12 *Corresponding author(s): François Clayer (francois.clayer@niva.no)

13

14 **Abstract**

15 The determination of dissolved gases (O₂, CO₂, CH₄, N₂O, N₂) in surface waters allows to estimate
16 biological processes and greenhouse gas fluxes in aquatic ecosystems. Mercuric chloride (HgCl₂) has
17 been widely used to preserve water samples prior to gas analysis. However, alternates are needed
18 because of the environmental impacts and prohibition of mercury. HgCl₂ is a weak acid and interferes
19 with dissolved organic carbon (DOC). Hence, we tested the effect of HgCl₂ and two substitutes
20 (copper (II) chloride – CuCl₂ and silver nitrate – AgNO₃), as well as storage time (24h to 3 months)
21 on the determination of dissolved gases in low ionic strength and high DOC water from a typical
22 boreal lake. Furthermore, we investigated and predicted the effect of HgCl₂ on CO₂ concentrations in
23 periodic samples from another lake experiencing pH variations (5.4–7.3) related to *in situ*
24 photosynthesis. Samples fixed with inhibitors generally showed negligible O₂ consumption. However,
25 effective preservation of dissolved CO₂, CH₄ and N₂O for up to three months prior to dissolved gas
26 analysis, was only achieved with AgNO₃. In contrast, HgCl₂ and CuCl₂ caused an initial increase in
27 CO₂ and N₂O from 24h to 3 weeks followed by a decrease from 3 weeks to 3 months. The CO₂
28 overestimation, caused by HgCl₂-acidification and shift in the carbonate equilibrium, can be
29 calculated from predictions of chemical speciation. Errors due to CO₂ overestimation in HgCl₂-
30 preserved water, sampled from low ionic strength and high DOC freshwater that are common in the
31 northern hemisphere, could lead to an overestimation of the CO₂ diffusion efflux by a factor of >20
32 over a month, or a factor of 2 over the ice-free season. The use of HgCl₂ and CuCl₂ for freshwater
33 preservation should therefore be discontinued. Further testing of AgNO₃ preservation should be
34 performed under a large range of freshwater chemical characteristics.

CO₂ overestimation from HgCl₂ fixation – Clayer et al.

35

36 **Key-words:** lake, greenhouse gases, water sample preservation, mercuric chloride, metal toxicity,
37 carbon dioxide

38 **Running tile:** CO₂ overestimation from HgCl₂ fixation

39 **1 Introduction**

40

41 The determination of dissolved gases by gas chromatography from water samples collected in the
42 field allows the estimation of biological processes in aquatic ecosystems such as photosynthesis and
43 oxic respiration (O₂, CO₂), denitrification (N₂, N₂O) and methanogenesis (CH₄). This technique is also
44 useful to test the calibration of *in-situ* sensors in long term deployment. However, the accuracy of this
45 approach largely depends on the effectiveness of sample fixation. In fact, the partial pressure of the
46 dissolved gases will continue to evolve in the water sample from the time of collection to the time of
47 analysis unless biological activity is prevented. This is an issue when field sites are far from
48 laboratory facilities, and when samples need to be stored until the end of the field season for more
49 efficient processing in large batches. Hence, before using a given biocide to preserve water samples, it
50 must be ensured that it is efficient in inhibiting biological activity without changing the sample's
51 chemistry.

52 Mercuric (II) chloride (HgCl₂) has been widely used as an inhibitor of the above-mentioned biological
53 processes to preserve water samples for the determination of dissolved CO₂ in seawaters (e.g.
54 Dickson, Sabine & Christian, 2007) and several dissolved gases in natural and artificial freshwater
55 bodies (e.g. O₂, CO₂, CH₄, N₂ and/or N₂O; Guérin et al., 2006; Hessen et al., 2017; Hilgert et al.,
56 2019; Okuku et al., 2019; Schubert et al., 2012; Xiao et al., 2014; Yan et al., 2018; Yang et al., 2015)
57 because it is extremely toxic at very low concentrations compared to other reagents (e.g. Horvatic &
58 Peršić, 2007; Hassen *et al.*, 1998). Worldwide efforts have sought to reduce the use of mercury
59 because it is considered toxic to the environment and exposure can severely affect human health
60 (Chen et al., 2018). Therefore, alternative preservation techniques to HgCl₂ amendment have been
61 tested for dissolved inorganic carbon (DIC) and δ¹³C-DIC such as acidification with phosphoric acid
62 (Taipale & Sonninen, 2009) or a combination of filtration and exposure to benzalkonium chloride or
63 sodium chloride (Takahashi *et al.*, 2019). At least two studies, one also including dissolved organic
64 carbon (DOC) and δ¹³C-DOC, showed that simple filtration (and cooling), fixation (precipitation) or
65 acidification were effective in preserving water samples (Wilson, Munizzi & Erhardt, 2020). Another
66 solution is to sample the headspace out in the field, and bring back gas samples (e.g., Cole et al.,
67 1994; Karlsson et al., 2013; Kling et al., 1991). However, these techniques were not tested for the
68 simultaneous determination of several dissolved gases, including CH₄ which is subject to rapid
69 degassing during handling or storage if samples are not preserved because of its low solubility in
70 water (Duan & Mao, 2006). In addition, some of the existing alternatives, such as filtration or field
71 headspace equilibration, are difficult to operate in remote areas in the field under harsh weather
72 conditions and prone to potential ambient air contamination. Solutions for water sample preservation
73 should therefore involve a minimum of manipulation steps in the field to avoid gas exchange with
74 ambient air. Biocide amendments into sealed water bottles appears as one of the most efficient

75 methods. Copper(II) chloride (CuCl₂) and silver nitrate (AgNO₃), the most toxic form of silver, are
76 relevant alternatives to HgCl₂ given their known toxicity (e.g., Ratte 2009; Amorim and Scott-
77 Fordsmand 2012) and wide application in water treatments and water purification (Larrañaga et al.,
78 2016; Nowack et al., 2011; NPIRS, 2023; Ullmann et al., 1985). Nevertheless, the efficiency of these
79 alternative biocides has never been tested for dissolved gas samples preservation.

80 The addition of HgCl₂ to water is known to produce hydrochloric acid through hydrolysis (Ciavatta &
81 Grimaldi, 1968) and to form complexes with many environmental ligands, both inorganic (Powell *et*
82 *al.*, 2004) and organic (Tipping, 2007; Foti *et al.*, 2009; Liang *et al.*, 2019; Chen *et al.*, 2017). The
83 complexation of Hg⁺ with the carboxyl or thiol groups of DOC in oxic environments could further
84 increase the concentration of H⁺ (Khwaja et al., 2006; Skyllberg, 2008). This acidification can be an
85 issue in poorly buffered water (low ionic strength) with high concentration of DOC where a shift in
86 the pH and carbonate equilibrium can be induced. In that case, the estimated CO₂ concentration would
87 be higher after HgCl₂ fixation than the *in situ* concentration, and if the shift in pH is not accounted for,
88 can result in an overestimation of dissolved CO₂ and bicarbonate concentrations. A similar
89 acidification effect is also expected with CuCl₂ amendments (Rippner et al., 2021), but not for AgNO₃
90 amendments. Such effects would not be expected in marine water due to the high ionic strength of the
91 water (Chou *et al.*, 2016) or freshwater with low pH (<5.5) under which conditions nearly all
92 dissolved inorganic carbon is CO₂ (Stumm & Morgan, 1981). Thus, there are clear limits of the
93 application of HgCl₂, and possibly CuCl₂, for freshwater sample preservation given its risk of leading
94 to overestimation of CO₂ and bicarbonate concentrations, in addition to exposing field workers to the
95 risks of its high toxicity.

96

97 Here we combine data from laboratory experiments (i) and field work (ii) to illustrate risks of mis-
98 estimation of dissolved gas concentrations in freshwaters with some preservatives and provide
99 recommendation for best practices in the field. First, we (i) performed some short-term and long-term
100 incubations of water from a typical heterotrophic unproductive boreal lake with circumneutral pH,
101 low ionic strength (poor buffering capacity) and high DOC concentration to test the effect of storage
102 time and different preservative amendments on the determination of five dissolved gases (O₂, CO₂,
103 CH₄, N₂ and N₂O) by headspace equilibration and gas chromatography. The preservatives were
104 mercuric chloride (HgCl₂) and two alternative inhibitors, chosen for their wide and effective
105 application in water treatments and water purification (copper (II) chloride – CuCl₂ and silver nitrate –
106 AgNO₃; Xu & Imlay, 2012; Rai, Gaur & Kumar, 1981). Unamended water samples, where only
107 ultrapure water was added, were also included for comparison. In addition, we (ii) analysed dissolved
108 CO₂ concentration data obtained from a typical productive boreal lake using two independent
109 methods, one by gas chromatography following HgCl₂ fixation, and one through dissolved inorganic

110 carbon determination without fixation. We show that the overestimation of dissolved CO₂
111 concentrations caused by HgCl₂ fixation can be predicted based on chemical equilibria.

112

113 **2. Methods**

114 2.1. Effects of storage time and inhibitors on the quantification of dissolved gases

115 *Study site and sampling*

116 Surface water was collected from Lake Svartkulp (59.9761313 N, 10.7363544 E; Southeast Norway)
117 north of Oslo, Norway, on the 4th of September 2019. A 5 L plastic bottle was gently pushed into the
118 water and progressively tilted to let the water flow into the bottles without bubbling. The bottle
119 aperture was covered with a 90 µm plankton net to avoid sampling large particles. This procedure was
120 repeated five times to yield a total water volume of 25 L. The 5 L water bottles were immediately
121 brought back to the lab. Upon arrival at the laboratory, after temperature equilibration, water from the
122 5 L bottles was slowly poured, to limit gas exchange with the ambient air, into a 25 L tank to provide
123 a single bulk sample to start the incubation experiment. Filtration, e.g., with 0.45 or 0.2 µm filters,
124 was avoided to minimize changes in dissolved gas concentrations (e.g., Magen et al., 2014). The
125 mixed water sample (25 L) was sub-sampled (0.5 L) for the determination of alkalinity (127 µmol L⁻¹)
126 ¹), pH (6.73), ammonium (3 µg N L⁻¹), nitrate (5 µg N L⁻¹), total N (230 µg N L⁻¹), phosphate (1 µg P
127 L⁻¹), total P (9 µg P L⁻¹) and TOC (8.9 mg C L⁻¹) all analysed by standard methods at the accredited
128 Norwegian Institute for Water Research (NIVA) lab (see Tab. S1). *In situ* temperature of the lake
129 water was measured with a handheld thermometer and was 18.5 °C. Note that particulate organic
130 carbon is a negligible fraction of TOC in Norwegian lake waters, representing on average less than
131 3% (de Wit et al., 2023).

132 Lake Svartkulp was selected for this experiment because it is representative of low ionic strength
133 Northern Hemisphere lakes, typically found in granitic bedrock regions in North-East America and
134 Scandinavia. It is a typical low-productivity, heterotrophic, slightly acidic to neutral, moderately
135 humic lake. Similar lakes are found in Southern Norway (de Wit et al., 2023), large parts of Sweden
136 (Valina et al. 2014), Finland, Atlantic Canada (Houle et al., 2022), Ontario, Québec, and North-East
137 USA (Skjelkvåle and de Wit 2011; Weyhenmeyer et al., 2019).

138 *Laboratory incubation experiment with different preservatives and storage times*

139 The experimental design involved to incubate 72 borosilicate glass bottles (120 mL) filled with lake
140 water from our 25 L bulk sample and submitted to four different treatments: addition of 240µL of a
141 preservative solution of (i) HgCl₂, (ii) CuCl₂ or a (iii) AgNO₃, or addition of 240 µL of (iv) MilliQ
142 water. The bottles amended with MilliQ water are hereafter referred to as “unfixed”. The 72 bottles

143 were divided into three groups which were incubated cold (+4°C) and dark for 24h, three weeks or
 144 three months respectively, before being processed for dissolved gas analysis by gas chromatography.
 145 These incubation times were selected to represent situations where samples are processed directly
 146 upon return to the laboratory (24h), or after medium (3 weeks) to long (3 months) -term storage,
 147 respectively. At each time point and for each treatment, a group of 6 bottles were further processed for
 148 dissolved gas analysis. Concentrations of O₂, N₂, N₂O, CO₂ and CH₄ were determined by gas
 149 chromatography (see below) using the headspace technique following Yang *et al.* (2015). pH was not
 150 measured at the end of the storage period.

151 In details, within 3h of lake water sampling, the 120mL bottles were gently filled with water from the
 152 mixed sample (25 L). Each 120mL bottle was slowly lowered into the water and progressively tilted
 153 to let the water flow into the bottle without bubbling. The bottle was then capped under water with a
 154 gas tight butyl rubber stopper after ensuring that there were no air bubbles in the bottle. The bottles
 155 were randomized prior to preservative or MilliQ amendment. The preservative solution or MilliQ
 156 amendment was pushed in each bottle with a syringe and needle through the rubber septum. To avoid
 157 overpressure, another needle was placed through septum at the same time, at least 2 cm above the
 158 other needle, to allow an equivalent volume of clean water to be released.

159 Stock solutions of HgCl₂, CuCl₂ and AgNO₃ were prepared according to Tab. 1 using high accuracy
 160 chemical equipment (e.g., high accuracy scale, volumetric flasks). The Ag (Silver nitrate EMSURE®
 161 ACS; Merck KGaA, Germany) Cu (Copper(II) chloride dihydrate; Merck Life Science ApS, Norway)
 162 and Hg (Mercury(II) chloride; undetermined) salts were dissolved in MilliQ ultrapure water (>18 MΩ
 163 cm). For measurement of CO₂ in seawater samples, the standard method involves poisoning the
 164 samples by adding a saturated HgCl₂ solution in a volume equal to 0.05-0.02% of the total volume
 165 (Dickson 2007). We used this as a starting point and added 0.02 % saturated HgCl₂ solution to 18
 166 bottles (240 µL of HgCl₂ 10× diluted saturated solution), resulting in a sample concentration of 14 µg
 167 HgCl₂ mL⁻¹ (51.6 µM; Tab. 1). Based on estimated toxicity relative to Hg (Deheyn et al., 2004; Halmi
 168 et al., 2019), the silver and copper salts were added in molar concentrations equal to two and three
 169 times the molar concentration of HgCl₂, respectively (Tab. 1), although it varies between species of
 170 microorganisms and environmental matrices (Hassen *et al.*, 1998; Rai, Gaur & Kumar, 1981).

171 **Table 1.** Stock and sample concentrations of HgCl₂, CuCl₂ and AgNO₃.

Salt	Stock solution	Sample concentration	Rationale
HgCl ₂	70 g/L (saturated)	14.0 µg/mL (51.6 µM)	Dickson, Sabine & Christian, 2007
CuCl ₂	131.9 g/L	26.4 µg/mL (154.7 µM)	3 × Hg
AgNO ₃	87.6 g/L	17.5 µg/mL (103.1 µM)	2 × Hg

172

173 *Additional 24h incubation experiment with different preservatives for pH measurements*

174 Since pH was not measured at the end of the first incubation experiment, we performed an additional
175 experiment to document any potential rapid (within 24h) impacts of preservative on pH. A total of 48
176 borosilicate glass bottles (120 mL) filled with lake water were submitted to the same four different
177 treatments as the first experiment described above: HgCl₂, CuCl₂, AgNO₃ or MilliQ water
178 amendments. To this end, a 20L water tank was filled with surface water from Lake Svartkulp on the
179 14th of December 2023. The water tank was immediately returned to the laboratory and left for 24h to
180 equilibrate to the room temperature. On December 15th, 120mL bottles were gently filled with water
181 from the bulk 20L sample, as described above. The bottles were randomized prior to preservative or
182 MilliQ amendment performed as described above. The bottles were then incubated at room
183 temperature for 2h or 24h. pH was measured in the initial unamended lake water, in 24 bottles opened
184 after 2h incubation, and in 24 bottles opened after 24h incubation. pH measurements were performed
185 with a WTW Multi 3620 pH meter calibrated using a two-point calibration at pH = 4 and pH = 7. All
186 pH measures were corrected for temperature. Water temperature of the water samples during pH
187 measurements ranged between 19.1 and 21.2°C.

188

189 2.2. Effects of HgCl₂ on dissolved CO₂ analyses over a range of pH values

190 *Study site and sampling*

191 Water samples were collected from Lake Lundebyvannet located southeast of Oslo (59.54911 N,
192 11.47843 E, Southeast Norway). Two sets of samples were taken from 1, 1.5, 2 and 2.5 m depth
193 using a water sampler once or twice a week between April 2020 and January 2021 for the
194 determination of (i) dissolved CO₂ by GC analysis following fixation with HgCl₂ and (ii) DIC
195 analysis with a TOC analyser. Samples for GC analysis were filled into 120 mL glass bottles (as
196 described above for the 72 incubation bottles), which were sealed with rubber septa under water
197 without air bubbles. Samples for GC analysis were preserved in the field by adding a half-saturated (at
198 20°C) solution of HgCl₂ (150 µL) through the rubber seal of each bottle using a syringe, as described
199 above the 72 incubation bottles, resulting in a concentration of 161 µM similar to previous studies
200 (Clayer et al., 2021; Hessen et al., 2017; Yang et al., 2015). Samples for DIC analysis were filled
201 without bubbles in 100 ml Winkler glass bottles that were sealed airtight directly after sampling.
202 These samples were not fixed in any way and were analysed by a TOC analyzer within two hours.
203 Lake water temperature and pH were measured *in-situ* using HOBO pH data loggers placed at 1, 1.5,
204 2 and 2.5 m (Elit, Gjerdrum, Norway).

205 Lake Lundebyvannet has a surface area of 0.4 km² and a maximum depth of 5.5 m. It often
206 experiences large blooms of *G. semen* over the summer between May and September (Hagman et al.,

207 2015; Rohrlack, 2020). The lake water is characterised by high and fluctuating concentrations of
208 humic substances (with DOC concentrations ranging from 8 to 28 mg C L⁻¹), ammonium (5 to 100 µg
209 N L⁻¹), nitrate (20 to 700 µg N L⁻¹), total N (average of 612 µg N L⁻¹), phosphate (2 to 4 µg P L⁻¹),
210 total P (average of 28 µg P L⁻¹; Rohrlack et al., 2020; Hagman et al., 2015), a fluctuating pH (from 5.5
211 to 7.3), weak ionic strength with alkalinity ranging between 30 and 150 µmol L⁻¹, and electric
212 conductivity varying from 40 to 70 µS cm⁻¹. For more details, see Rohrlack *et al.* (2020).

213 Lake Lundebyvannet was selected for this experiment because it is representative of productive, low-
214 ionic strength Northern Hemisphere lakes typically found in the southern part of granitic bedrock
215 regions in North-East America and Scandinavia.

216 2.3. Analytical chemistry

217 *Gas chromatography*

218 Headspace was prepared by gently backfilling sample bottles with 20–30 mL helium (He; 99,9999%)
219 into the closed bottle while removing a corresponding volume of water. Care was taken to control the
220 headspace pressure within 5% of ambient and a slight He overpressure was released before
221 equilibration. The bottles were shaken horizontally at 150 rpm for 1 h to equilibrate gases between
222 sample and headspace. The temperature during shaking was recorded by a data logger. Immediately
223 after shaking, the bottles were placed in an autosampler (GC-Pal, CTC, Switzerland) coupled to a gas
224 chromatograph (GC) with He back-flushing (Model 7890A, Agilent, Santa Clara, CA, US).
225 Headspace gas was sampled (approx. 2 mL) by a hypodermic needle connected to a peristaltic pump
226 (Gilson Minipuls 3), which connected the autosampler with the 250 µL heated sampling loop of the
227 GC.

228 The GC was equipped with a 20-m wide-bore (0.53 mm) Poraplot Q column for separation of CH₄,
229 CO₂ and N₂O and a 60 m wide-bore Molsieve 5Å PLOT column for separation of O₂ and N₂, both
230 operated at 38°C and with He as carrier gas. N₂O and CH₄ were measured with an electron capture
231 detector run at 375°C with Ar/CH₄ (80/20) as makeup gas, and a flame ionization detector,
232 respectively. CO₂, O₂, and N₂ were measured with a thermal conductivity detector (TCD). Certified
233 standards of CO₂, N₂O, and CH₄ in He were used for calibration (AGA, Germany), whereas air was
234 used for calibrating O₂ and N₂. The analytical error for all gases was lower than 2%. For the Lake
235 Lundebyvannet time series, CO₂ was separated from other gases using the 20 m wide-bore (0.53 mm)
236 Poraplot Q column while the other gases were not measured.

237 The results from gas chromatography give the relative concentration of dissolved gases (in ppm) in
238 the headspace in equilibrium with the water. For the lab experiment with Svartkulp samples (section
239 2.1), the concentration of dissolved gases in the water at equilibrium with the headspace were
240 calculated from the temperature corrected Henry constant in water using Carroll, Slupsky and Mather

241 (1991) for CO₂, Weiss and Price (1980) for N₂O, Yamamoto, Alcauskas and Crozier (1976) for CH₄,
 242 Millero, Huang and Laferiere (2002) for O₂, Hamme and Emerson (2004) for N₂. For the Lake
 243 Lundebyvannet time series (section 2.2), the concentration of CO₂ in the water samples were
 244 determined using temperature-dependent Henry's law constants given by Wilhelm, Battino and
 245 Wilcock (1977). The quantities of gases in the headspace and water were summed to find the
 246 concentrations and partial pressures of dissolved gases from the water collected in the field as follows:

$$247 \quad [gas] = \frac{p_{gas}HV_{water} + \frac{p_{gas}V_{headspace}}{RT}}{V_{water}} \quad (\text{Eq. 1})$$

248 where [gas] is the gas aqueous concentration, p_{gas} is the gas partial pressure, H is the Henry constant,
 249 V_{water} is the volume of water sample during headspace equilibration, $V_{headspace}$ is the headspace gas
 250 volume during equilibration, R is the gas constant and T the temperature during headspace
 251 equilibration (recorded during shaking). The calculations were similar to Yang *et al.* (2015).

252

253 *DIC analyses*

254 DIC analysis was performed for the Lake Lundebyvannet time series using a Shimadzu TOC-V CPN
 255 (Oslo, Norway) instrument equipped with a non-dispersive infrared (NDIR) detector with O₂ as a
 256 carrier gas at a flow rate of 100 mL min⁻¹. Two to three replicate measurements were run per sample.
 257 The system was calibrated using a freshly prepared solution containing different concentrations of
 258 NaHCO₃ and Na₂CO₃. CO₂ concentrations in water samples ($[CO_2]$) were calculated on the bases of
 259 temperature, pH and DIC concentrations as follows (Rohrlack *et al.*, 2020):

$$260 \quad [CO_2] = \frac{[H^+]^2 C_T}{Z} \quad (\text{Eq. 2})$$

261 where $[H^+]$ is the proton concentration (10^{-pH}), C_T is the dissolved inorganic carbon concentration
 262 and Z is given by:

$$263 \quad Z = [H^+]^2 + K_1[H^+] + K_1K_2 \quad (\text{Eq. 3})$$

264 where K_1 and K_2 are the first and second carbonic acid dissociation constant adjusted for temperature
 265 ($pK_1 = 6.41$ and $pK_2 = 10.33$ at 25°C; Stumm & Morgan, 1996).

266

267 2.4. Data analysis

268 *pCO₂ and saturation deficit*

269 Lake Lundebyvannet CO₂ concentrations provided by GC and DIC analyses were converted to pCO₂
 270 (in µatm) as follows:

$$pCO_2 = \frac{[CO_2]}{0.987 \times K_H P_{atm}} \quad (\text{Eq. 4})$$

where K_H is Henry constant for CO₂ adjusted for in-situ water temperature (Stumm & Morgan, 1996) and P_{atm} is the atmospheric pressure in bar approximated by:

$$P_{atm} = (1013 - 0.1 \times \text{altitude}) \times 0.001 \quad (\text{Eq. 5})$$

where *altitude* is the altitude above sea level of Lake Lundebyvannet (158 m). Finally, the CO₂ saturation deficit (Sat_{CO_2} in μatm) was given by

$$Sat_{CO_2} = pCO_2 - [CO_2]_{air} \quad (\text{Eq. 6})$$

where $[CO_2]_{air}$ is the pCO₂ in the air (416 μatm for 2020 in Southern Norway retrieved from EBAS database; NILU, 2022; Tørseth et al., 2012). Sat_{CO_2} gives the direction of CO₂ flux at the water-atmosphere interface, and its product with gas transfer velocity determine the CO₂ flux at the water-atmosphere interface, i.e., whether lake ecosystems are sink ($Sat_{CO_2} < 0$) or source ($Sat_{CO_2} > 0$) of atmospheric CO₂.

283

284 *Statistical analyses*

285 The effect of storage time and treatment on five dissolved gases (O₂, N₂, CO₂, CH₄, N₂O) from the
286 Lake Svartkulp samples was tested with a two-way ANOVA at an alpha level adapted using the
287 Bonferroni correction for multiple testing, i.e., $\alpha=0.05/5=0.01$. To evaluate the impact of Hg fixation
288 on Lake Lundebyvannet samples, $[CO_2]$ values determined by headspace equilibration and GC
289 analysis of HgCl₂-fixed samples were compared with those calculated from DIC measurements of
290 unfixed samples with a paired t-test.

291 A regression analysis was performed to describe the overestimation of CO₂ concentrations caused by
292 HgCl₂ fixation in Lake Lundebyvannet samples as a function of pH. The total CO₂ concentration in
293 the HgCl₂-fixed samples ($[CO_2]_{HgCl_2}$) can be expressed as:

$$[CO_2]_{HgCl_2} = [CO_2]_i + [CO_2]_{ex} \quad (\text{Eq. 7})$$

295 where $[CO_2]_i$ is the initial CO₂ concentration prior to HgCl₂ fixation, i.e., CO₂ concentration in the
296 unfixed samples, and $[CO_2]_{ex}$ is the excess CO₂ concentration caused by a decrease in pH following
297 HgCl₂ fixation. The relative CO₂ overestimation (E in %) is given by:

$$E = \frac{[CO_2]_{HgCl_2} - [CO_2]_i}{[CO_2]_i} = \frac{[CO_2]_{ex}}{[CO_2]_i} \quad (\text{Eq. 8})$$

298

299 The impact of pH (or $[H^+]$) on E was mathematically described by running a regression analysis
300 using MATLAB®. The *fminsearch* MATLAB function from the Optimization toolbox was used to
301 find the minimum sum of squared residuals (SSR) for functions of the form of: $E = A/[H^+]$ or $E =$
302 $A \times 10^{-B \times pH}$. For each optimal solution, the root-mean-square error (RMSE) and coefficient of
303 determination (R^2) were calculated against observed values of E , i.e., values of E determined
304 empirically from observed $[CO_2]_i$ and $[CO_2]_{ex}$.

305

306 *Chemical speciation, saturation-index calculations, and prediction of CO₂ overestimation*

307 The speciation of solutes and saturation index values (SI) of selected minerals were calculated with
308 the program PHREEQC developed by the USGS (Parkhurst & Appelo, 2013), neglecting the effect of
309 dissolved organic matter. This was used to assess the impact of the addition of preservative on shifting
310 the carbonate equilibrium as well as dissolved inorganic carbon losses due to carbonate mineral
311 precipitation. For each PHREEQC simulation, two files, respectively the database (with input
312 reactions) and input files, were used to define the thermodynamic model and the type of calculations
313 to perform. The database of MINTQA2 (e.g., *minteq.dat*, Allison et al., 1991) was used to describe
314 the chemical system because it includes, inter alia, reactions and constants for Ag, Cu and Hg
315 complexation with Cl, NO₃ and carbonates. In total, three simulations were run representing the
316 addition of each preservative solution to sample water from Lake Svartkulp. The input files described
317 the composition of two aqueous solutions: (i) the preservative solution assumed to contain only the
318 preservative and (ii) sample water from Lake Svartkulp with observed major element concentrations
319 (pH, Al, Ca, Cl, Cu, Fe, Mg, Mn, N as nitrate, K, Na, S as sulfate, Zn; Tab. S1) and Hg and Ag
320 concentration assumed to be 10⁻⁵ mg/L. The output file provided the activities of the various solutes in
321 the preserved samples, i.e., simulating the mixing of 120 mL of lake water with 240 µL of the AgNO₃,
322 CuCl₂ and HgCl₂ preservative solutions, as described in section 2.1. This procedure allows to estimate
323 the pH of the preserved samples as well as SI for various mineral phases. The SI is calculated by
324 PHREEQC comparing the chemical activities of the dissolved ions of a mineral (ion activity product,
325 IAP) with their solubility product (Ks). When SI > 1, precipitation is thermodynamically favourable.
326 However, PHREEQC does not give information about precipitation kinetics.

327 PHREEQC was also used to estimate the decrease in pH caused by adding 150 µL of a half-saturated
328 HgCl₂ solution to Lake Lundebyvannet samples prior to GC analyses, as described in section 2.2. In
329 absence of data on the chemical composition of Lake Lundebyvannet, we assumed that it had the
330 same composition as Lake Svartkulp water samples. This assumption is supported by the fact that
331 waters from both lakes have circumneutral pH, low ionic strength (poor buffering capacity) and high
332 DOC concentration and would therefore behave similarly in presence of acids. Briefly, for each 0.1
333 pH value between pH of 5.4 and 7.3, the carbonate alkalinity was first adjusted by increasing HCO₃

334 concentrations in the input files for PHREEQC to confirm that the water was at equilibrium at the
 335 given pH value. Then, the effect of adding 150µL of a half-saturated HgCl₂ solution was simulated as
 336 described above for Lake Svartkulp. Knowing the new equilibrated pH, after addition of HgCl₂, the
 337 overestimation of CO₂ concentration in Hg-fixed samples relative to unfixed samples (E , described in
 338 Eq. 8 above) can be predicted as described below.

339 Adapting Eq. (2), we obtain:

$$340 \quad [CO_2]_{HgCl_2} = \frac{[H^+]_{HgCl_2}^2 C_T}{Z_{HgCl_2}} \quad (\text{Eq. 9})$$

341 and

$$342 \quad [CO_2]_i = \frac{[H^+]_i^2 C_T}{Z_i} \quad (\text{Eq. 10})$$

343 where $[H^+]_i$ is the proton concentration measured in the initial water samples prior to HgCl₂ fixation,
 344 and $[H^+]_{HgCl_2}$ is the proton concentration estimated by PHREEQC following HgCl₂ fixation, and
 345 similarly for Z_i and Z_{HgCl_2} from Eq. (3). Combining Eqs. (7), (9) and (10) we obtain:

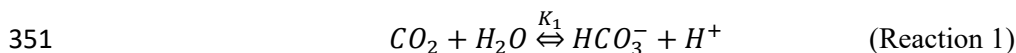
$$346 \quad [CO_2]_{ex} = C_T \left(\frac{[H^+]_{HgCl_2}^2}{Z_{HgCl_2}} - \frac{[H^+]_i^2}{Z_i} \right) \quad (\text{Eq. 11})$$

347 Hence:

$$348 \quad E = \frac{[CO_2]_{ex}}{[CO_2]_i} = \frac{\left(\frac{[H^+]_{HgCl_2}^2}{Z_{HgCl_2}} - \frac{[H^+]_i^2}{Z_i} \right)}{\frac{[H^+]_i^2}{Z_i}} \quad (\text{Eq. 12})$$

349

350 Alternatively, E can also simply be predicted based on the carbonic acid dissociation:



352 At equilibrium, we have:

$$353 \quad K_1 = \frac{[HCO_3^-][H^+]}{[CO_2]} \quad (\text{Eq. 13})$$

354 When pH is decreased upon addition of HgCl₂, a fraction (α) of the initial bicarbonate concentration
 355 $[HCO_3^-]_i$ is turned into CO₂. This fraction, expressed as $[CO_2]_{ex}$ in Eq. (7) above, can be estimated
 356 with Eq. 13 as follows:

$$357 \quad [CO_2]_{ex} = \alpha [HCO_3^-]_i = \frac{\alpha K_1 [CO_2]_i}{[H^+]_i} \quad (\text{Eq. 14})$$

358 Introducing the expression of $[CO_2]_{ex}$ from Eq. 14 into Eq. 8 yields:

$$359 \quad \frac{[CO_2]_{ex}}{[CO_2]_i} = E = \frac{\alpha K_1}{[H^+]_i} \quad (\text{Eq. 15})$$

360 When the decrease in pH, or acidification, is greater than the buffering capacity of the water: $\alpha = 1$.

361 The value of α cannot exceed 1 because the amount of CO₂ produced by a decrease in pH cannot

362 exceed the amount of HCO_3^- initially present. In all the other cases, we have: $\alpha < 1$. For both

363 predictions of E , i.e., with Eqs. 12 and 15, the root-mean-square error (RMSE) and coefficient of

364 determination (R^2) were calculated.

365 Finally, additional sources of CO₂ overestimation were investigated by analysing the residuals of the

366 model described by Eq. 12, i.e., the difference between E predicted with Eq. 12 and E determined

367 empirically with Eq. 8. Briefly, residuals were plotted against pH and *in situ* temperature. Residuals

368 were separated in two groups based on the empirical value of $[HCO_3^-]_i - [CO_2]_{ex}$, i.e., the first group

369 had values of $[HCO_3^-]_i - [CO_2]_{ex} \geq a$ while the second group had values of $[HCO_3^-]_i - [CO_2]_{ex} \leq$

370 $-a$ where different values for a were used: 20, 10 or 5 μM . The justification for separating residuals

371 in two groups is that: (i) the first group represents samples for which bicarbonate alkalinity in the

372 original sample is, as expected, higher than CO₂ overestimation after HgCl₂-fixation, while (ii) the

373 second group represents samples for which bicarbonate alkalinity is not sufficient to explain CO₂

374 overestimation after HgCl₂-fixation.

375

376 *CO₂ diffusion fluxes from Lake Lundebyvannet*

377 The diffusive flux of CO₂ (F_{CO_2} in mol m⁻² d⁻¹) from Lake Lundebyvannet surface water was

378 estimated according to:

$$379 \quad F_{CO_2} = \frac{k_{CO_2}([CO_2] - [CO_2]_{eq})}{1000} \quad (\text{Eq. 16})$$

380 where k_{CO_2} is the CO₂ transfer velocity in m d⁻¹, $[CO_2]$ is the surface water CO₂ concentration (μM),

381 and 1000 is a factor to ensure consistency in the units and $[CO_2]_{eq}$ is the theoretical water CO₂

382 concentration (μM) in equilibrium with atmospheric CO₂ concentration calculated with Eq. (3) and

383 pCO₂ of 416 μatm (see above).

384 The CO₂ transfer velocity (k_{CO_2}) was estimated as follows (Vachon & Prairie, 2013):

$$385 \quad k_{CO_2} = k_{600} \left(\frac{600}{Sc_{CO_2}} \right)^{-n} \quad (\text{Eq. 17})$$

386 where k_{600} is the gas transfer velocity (m d⁻¹) estimated from empirical wind-based models and Sc_{CO_2}

387 is the CO₂ Schmidt number for in situ water temperature (unitless; Wanninkhof, 2014). We used n

388 values of 0.5 or 2/3 when wind speed was below or above 3.7 m s⁻¹, respectively (Gu erin et al., 2007).
 389 Empirical k_{600} models included those from Cole & Caraco (1998; $k_{600} = 2.07 + 0.215U_{10}^{1.7}$),
 390 Vachon & Prairie (2013; $k_{600} = 2.51 + 1.48U_{10} + 0.39U_{10} \log_{10} LA$) and Crusius & Wanninkhof
 391 (2003; power model: $k_{600} = 0.228U_{10}^{2.2} + 0.168$ in cm h⁻¹). U_{10} and LA refer to mean wind speed at
 392 10 m in m s⁻¹ and lake area in km², respectively. Sub-hourly U_{10} data for 2020 was retrieved from a
 393 weather station of the Norwegian Meteorological Institute located 1.5 km west of Lake
 394 Lundebyvannet (station name: E18 Melleby; ID: SN 3480; 59.546 N, 11.4535E) using the Frost
 395 application programming interface (*Frost API*, 2022). Daily, monthly, and yearly (only covering the
 396 ice-free season: April-November) F_{CO_2} was estimated using Eq. (12). Daily [CO₂] was interpolated
 397 from weekly data using a modified Akima spline (makima spline in Matlab® based on Akima, 1974).
 398 This interpolation method is known to avoid excessive local undulations.

399 3. Results

400 3.1. Effects of preservatives and storage time on dissolved gases

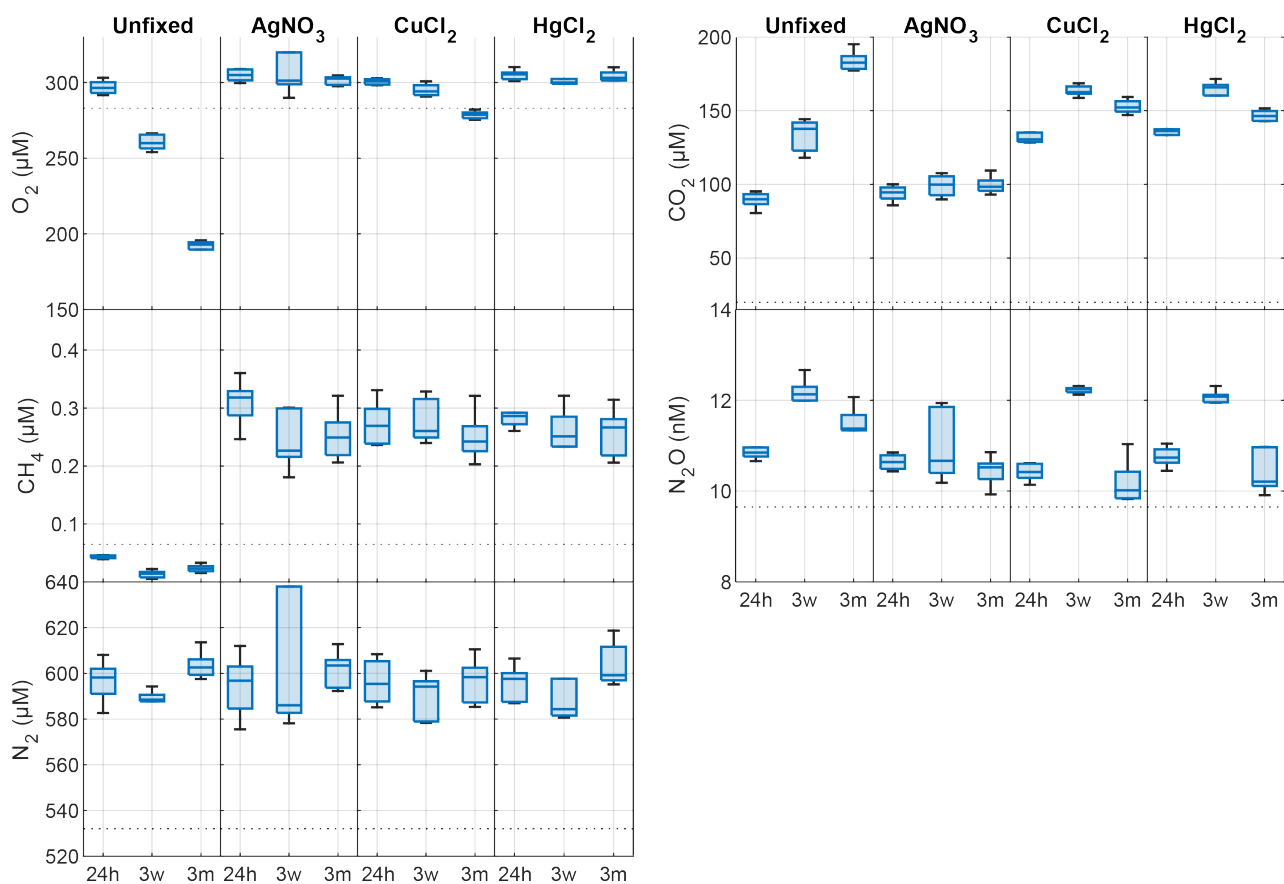
401 In the unfixed samples from Lake Svartkulp, the concentration of O₂ declined while CO₂ increased
 402 over time in a close to 1:1 molar ratio, likely reflecting the effect of microbial respiration activity and
 403 mineralisation of organic matter (Fig. 1, Tab. S2). Concentration of O₂ in the unfixed decreased from
 404 near 300 to below 200 µM (Fig. 1). In the presence of inhibitors, O₂ concentrations tended to be
 405 slightly higher at t=24h and remained constant or declined only slightly over time to generally remain
 406 at or above saturation (280 to 300 µM). Thus, the inhibitors were effective in reducing oxic
 407 respiration.

408 The concentration of CO₂ in the presence of AgNO₃ at t = 24h was not significantly different to the
 409 unfixed at t = 0 (Fig 1; paired t-test, $P > 0.1$). At t = 24h, CO₂ concentrations were however much
 410 higher in the presence of HgCl₂ (135 µM) or CuCl₂ (131 µM) than in the unfixed (89 µM; Fig 1, Tab.
 411 S2). The CO₂ further increases from 130 µM to ~160 µM after 3 weeks in both sample sets preserved
 412 with HgCl₂ and CuCl₂ while a decrease in O₂ is less pronounced for samples fixed with CuCl₂ and
 413 completely absent for samples fixed with HgCl₂. Overall, the addition of HgCl₂ or CuCl₂ following
 414 sampling increased CO₂ concentrations by 47% after 24h compared to the unfixed and caused further
 415 changes over the three-month storage time, while preservation with AgNO₃ yielded CO₂
 416 concentrations consistent with the unfixed and caused negligible changes over time (Fig. 1; paired t-
 417 test, $P > 0.1$).

418 The concentration of CH₄ across all samples ranged between 0.017 and 0.377 µM (Fig. 1), as
 419 expected two orders of magnitude smaller than CO₂. At t = 24h, the concentration of CH₄ was over
 420 0.2 µM in the presence of inhibitors while it was below saturation in the unfixed (0.03 µM; Fig. 1).

CO₂ overestimation from HgCl₂ fixation – Clayer et al.

421 CH₄ oversaturation in the preserved samples persisted after three weeks and three months of storage
422 and CH₄ concentration remained unchanged (Fig. 1, Tab. S2).



423

424 **Fig 1.** Changes in dissolved O₂, CO₂, CH₄, N₂O and N₂ concentrations (nM or µM) in the absence
 425 (unfixed) and presence of different preservatives (AgNO₃, CuCl₂, HgCl₂) at three times (24h, 24h
 426 after incubation start; 3w, three weeks after collection; 3m, three months after collection). The
 427 horizontal dotted line is the saturated gas concentration corresponding to 100% gas saturation at *in*
 428 *situ* lake temperature. Box plots show the median, 25th and 75th percentiles and the whiskers display
 429 all data coverage.

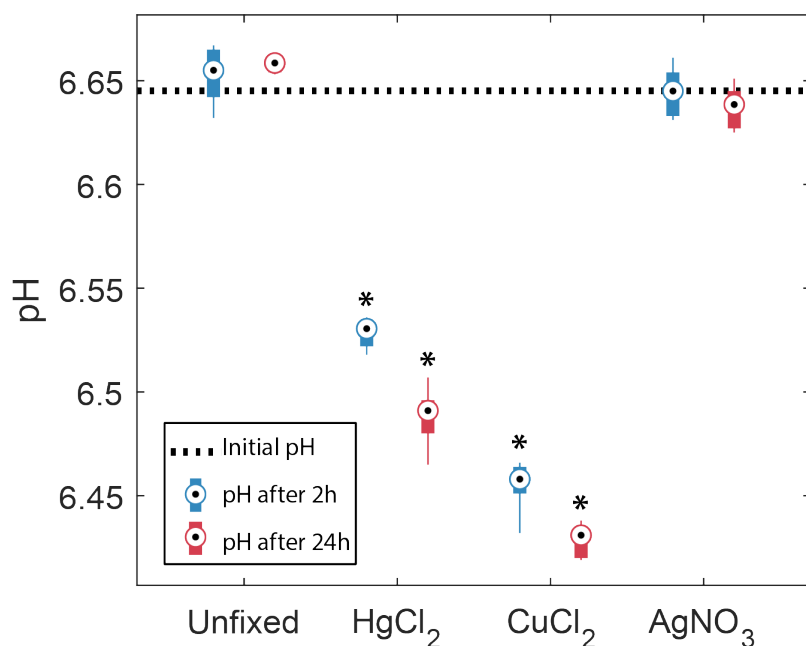
430 The concentration of N₂O ranged between 9.8 and 12.7 nM with only samples preserved with AgNO₃
 431 showing negligible changes over time (Fig. 1; paired t-test, P>0.1). All the other samples showed
 432 consistent patterns with storage time. N₂O concentrations initially increased within the first 3 weeks,
 433 followed by a decrease after 3 months.

434 The changes in N₂ were likely within handling and analytical errors and not different in the presence
 435 or absence of inhibitors (Fig. 1; Tab. S2; paired t-test, P>0.1).

436

437 3.2. Effects of preservatives on pH

438 In the samples amended with ultrapure water or AgNO₃, the pH did not show any significant changes
 439 after 2h or 24h. In contrast, both groups with HgCl₂ and CuCl₂ amendments show significant
 440 decreases of pH after 2h, -0.12 and -0.19, respectively, and 24h, -0.16 and -0.21, respectively. In
 441 addition, they showed a significant decrease in pH from 2h to 24h. Samples amended with CuCl₂
 442 show that strongest decrease in pH.



443

444 **Fig 2.** Changes in pH in the absence (unfixed) and presence of different preservatives (AgNO₃, CuCl₂,
 445 HgCl₂) at two times, 2h and 24h after the start of the incubation. The horizontal dotted line represents
 446 the initial pH of the bulk water sample. Box plots show the median, 25th and 75th percentiles and the
 447 whiskers display all data coverage of the 6 replicates. Stars indicate groups that are significantly
 448 different from each other and from the initial pH (two-way ANOVA).

449 3.3. Contrasting impacts of HgCl₂, CuCl₂ and AgNO₃ on dissolved CO₂ estimation revealed by
 450 chemical speciation modelling

451 The PHREEQC simulation of unpreserved samples, based on concentrations of all major elements
 452 (Tab. S1), predicted a pH of 6.72 (Tab. 2) which is very close to the measured pH of 6.73 (Tab. S1).
 453 This suggests that chemical information provided to PHREEQC is likely sufficient to describe the
 454 system, without having to invoke more complex reactions with dissolved organic matter. The addition
 455 of HgCl₂ and CuCl₂ both caused a significant decrease in pH to 6.40 and 6.45, respectively (Tab. 2).
 456 In absence of preservatives, none of the common carbonate minerals, including calcite, were
 457 associated with a saturation index higher than 1, i.e., dissolution was thermodynamically favourable
 458 for all these minerals and no DIC loss was expected (Tab. 2). However, upon addition of HgCl₂ or
 459 CuCl₂, some carbonate minerals, e.g., HgCO₃ or malachite and azurite, respectively, were expected to
 460 spontaneously precipitate given their relatively high saturation index values.

461 **Table 2.** pH and saturation indices of selected carbonate minerals estimated by PHREEQC for the
 462 unpreserved and preserved samples

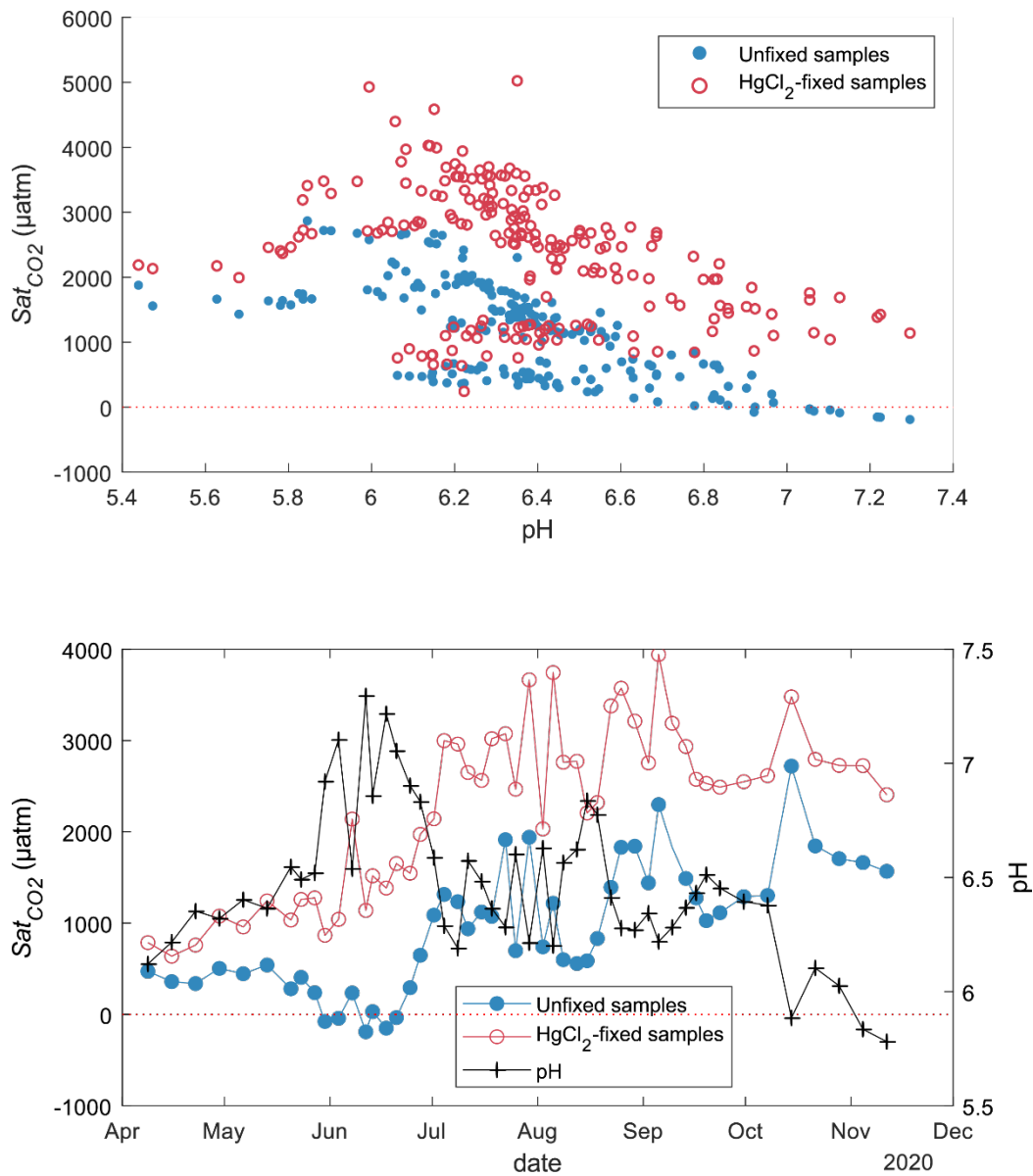
Preservatives	pH	Saturation indices			
		HgCO ₃	Cu ₂ (OH) ₂ CO ₃ - Malachite	Cu ₂ (OH) ₂ CO ₃ - Azurite	Ag ₂ CO ₃
Unfixed	6.72	-2.31	-4.96	-8.71	-16.42
HgCl ₂	6.40	3.64	-5.89	-10.10	-17.20
CuCl ₂	6.45	-2.55	2.26	2.11	-17.44
AgNO ₃	6.71	-2.31	-4.97	-8.73	-4.33

463

464 3.3. Effects of HgCl₂ on dissolved CO₂ concentration under a range of pH

465 CO₂ concentrations in unfixed water samples from Lake Lundebyvannet were significantly lower than
 466 in the HgCl₂-fixed samples (mean difference: 52 μM; paired t-test; P<0.0001; Tab. 3). Fixation with
 467 HgCl₂ caused a general overestimation of CO₂ concentration and the saturation deficit (Fig. 3), thus
 468 missing out events of CO₂ influx (carbon sink) under high photosynthesis activity (high pH; Fig. 3).
 469 In parallel, PHREEQC predicted a decrease of 0.6 to 1.8 units of pH related to HgCl₂ addition (Fig.
 470 S1).

471



472

473 **Figure 3.** CO₂ saturation deficit in Lake Lundebyvannet as a function of in situ pH for all unfixed
 474 (obtained from DIC analysis) and HgCl₂-fixed (obtained from GC analysis) samples (top panel).
 475 Timeseries of pH and CO₂ saturation deficit of surface water (1-m deep) for unfixed and HgCl₂-fixed
 476 samples (bottom panel).

477 **Table 3.** CO₂ concentrations ([CO₂], μM) and diffusion fluxes (F_{CO₂}, mol m⁻² d⁻¹) from Lake
 478 Lundebyvannet estimated from HgCl₂-fixed and unfixed samples following Cole and Caraco (1998).
 479 Ice-free season spans April to November. Data are also shown in Fig. 5.

Preservatives		Apr.	May	Jun.	Jul.	Aug.	Sep.	Oct.	Nov.	Ice-free season
[CO ₂]	None	45	39	19	68	59	85	123	120	67
	HgCl ₂	68	75	74	133	130	149	179	178	121
	Diff (%)	+50	+93	+296	+96	+119	+75	+45	+49	+82
F _{CO₂}	None	0.10	0.07	0.01	0.15	0.11	0.23	0.37	0.48	0.17
	HgCl ₂	0.20	0.21	0.16	0.34	0.29	0.47	0.57	0.77	0.35
	Diff (%)	+97	+188	+2163	+130	+162	+99	+55	+62	+108

480 The pH value of water samples from Lake Lundebyvannet varied between 5.4 and 7.3 (Fig 3 and 4),
 481 mainly due to marked variations in phytoplankton photosynthetic activity (Rohrlack et al., 2020). The
 482 relative overestimation of CO₂ (*E*) follows an exponential increase with pH and is well reproduced by
 483 a simple exponential function ($2.56 \times 10^{-5} \times 10^{1.015 \times pH}$, RMSE=44%, R²=0.81, p<0.0001; Fig. 4).

484

485 4. Discussion

486 Prior to using dissolved gas concentrations in freshwater to estimate the magnitude of biological
 487 aquatic processes such as photosynthesis and oxic respiration, denitrification and methanogenesis, we
 488 must ensure that biological activity between sampling and laboratory analyses was efficiently
 489 inhibited without significant impacts on the sample's chemistry. Here we report a unique dataset on
 490 the impact of three preservatives on water samples from a typical low-ionic strength, unproductive
 491 boreal lake to inform on potential risks of mis-estimation of dissolved gas concentrations. We further
 492 show, using CO₂ concentration data from a typical productive boreal lake, that using HgCl₂ can lead
 493 to negligence of the role of photosynthesis in lake C cycling.

494 4.1 Best preservative for the determination of dissolved gas concentrations

495 Given that none of the four treatments (unfixed, HgCl₂, CuCl₂ or AgNO₃) applied to Lake Svartkulp
 496 water samples during the 3-month incubation offer an independent control, a first challenge is to
 497 determine which of the treatment represent the most realistic dissolved gas concentrations close to
 498 real condition. For CO₂ and O₂, a few studies have used unfixed samples (only preserved dark at
 499 +4°C) up to 48h after sampling to determine CO₂ or DIC concentrations (e.g., Sobek et al. 2003,
 500 Kocic et al., 2015). So, the CO₂ and O₂ concentrations in the unfixed samples collected after 24h
 501 incubation are the most representative of the initial real concentrations. Biological activity might have
 502 had an impact, but this is likely negligible over the first 24h. In addition, the fact that the CO₂ and O₂

503 concentrations in the samples fixed with AgNO₃ after 24h, three weeks and three months are equal to
504 those from unfixed samples after 24h (Fig. 1) confirms that the unfixed samples after 24h can be used
505 as a control. In fact, only samples fixed with AgNO₃ are trustful given the expected toxicity of Ag, the
506 absence of impact on pH (Fig. 2), and unchanged concentrations over the three-month experiment for
507 all gases. Similarly, N₂O and N₂ concentrations in the unfixed samples after 24h can be used as
508 control. However, for CH₄, Fig. 1 shows that already after 24h, the CH₄ concentration in the unfixed
509 samples is below atmospheric saturation while it is consistently much higher in all three sets of fixed
510 samples. Boreal lakes are typically over saturated with respect to CH₄ (Valiente et al., 2022) and it is
511 very unlikely that CH₄ could have been produced in lake water incubated under high concentration of
512 oxygen and toxic preservatives. Hence, unfixed samples do not represent real CH₄ concentrations.
513 These observations are all consistent with the fact that the three preservatives were effective in
514 preserving CH₄ from oxidation. Even at t = 24h, preservatives are required to preserve CH₄ in oxic
515 samples. In fact, oxic methanotrophy typically show rates in the order of μM day⁻¹ (Thottathil et al.,
516 2019; van Grinsven et al., 2021). Hence, a CH₄ consumption of 0.3 μM within 24h in the unfixed
517 water samples is realistic (Fig. 1).

518 In summary, preservation with AgNO₃ is the only method that offered robust determination of all five
519 dissolved gases with negligible changes in concentration over time.

520 4.2 Risks of mis-estimating dissolved gas concentration with HgCl₂ and CuCl₂ preservation

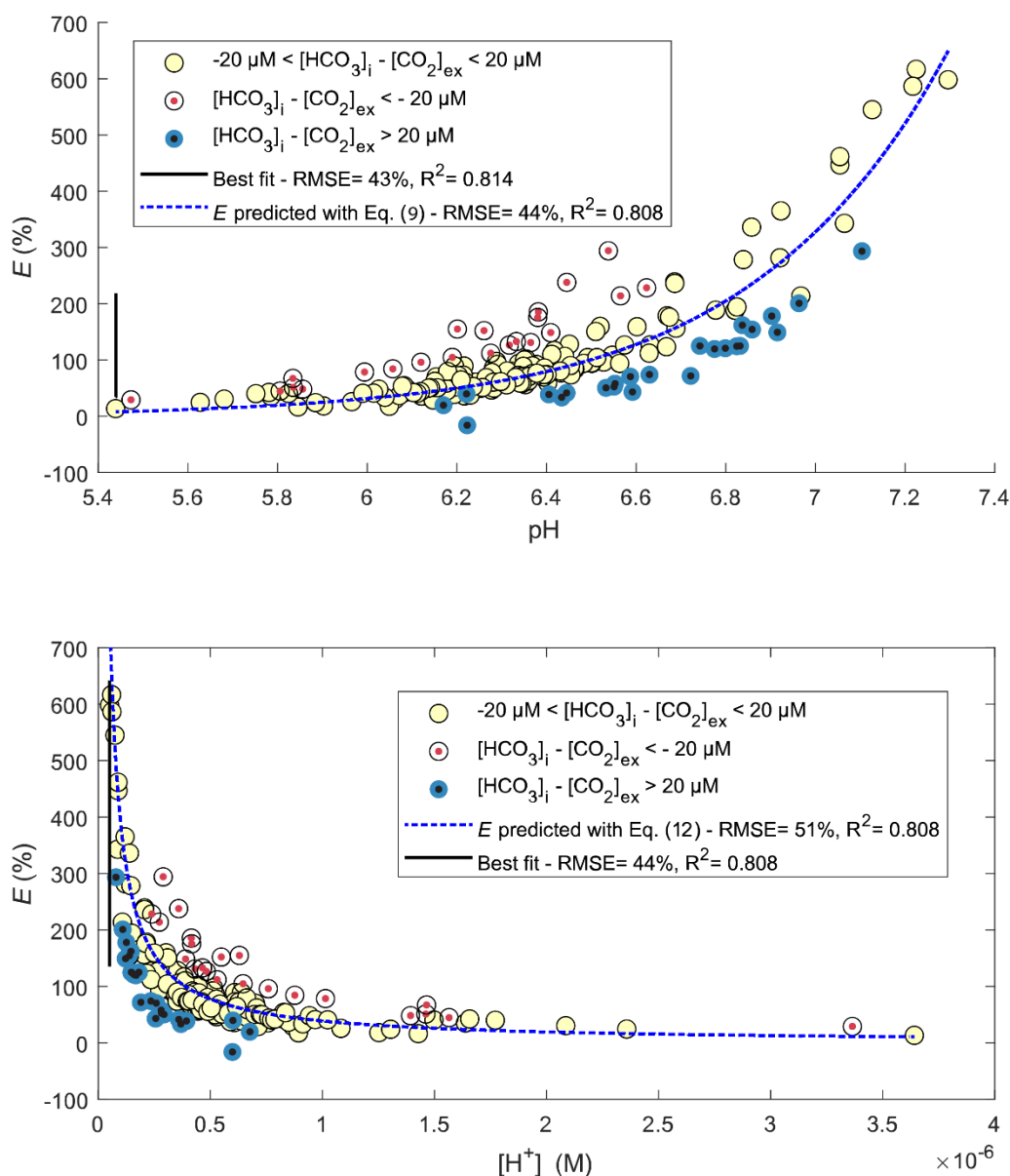
521 Both sets of samples preserved with either HgCl₂ and CuCl₂ showed CO₂ concentrations that were
522 much higher than the unfixed (after 24h) or the AgNO₃-fixed samples. This is due to an acidification
523 of the poorly buffered (alkalinity 127 μM) and near neutral water (pH=6.73), shifting the carbonate
524 equilibrium from HCO₃⁻ to CO₂ as also shown by Borges et al. (2019). In fact, a rapid decrease in pH
525 was observed upon HgCl₂ and CuCl₂ amendments (Fig. 2). The increase of CO₂ from about 130 μM
526 to ~160 μM after 3 weeks in both sample sets preserved with HgCl₂ and CuCl₂ is not mirrored by a
527 similar decrease in O₂ (Fig. 1) This suggests that oxic respiration is not the main source for this
528 additional 30 μM of CO₂ but rather points towards additional acidification of the samples caused, e.g.,
529 by kinetically controlled complexation of Hg²⁺ with dissolved organic matter (Miller et al., 2009). In
530 fact, the relatively slow complexation of Hg²⁺ with organic thiol groups can release two protons
531 (Skylberg, 2008) and up to three, with some participation of a third weak-acid group (Khwaja et al.,
532 2006). The transient nature of acidification caused by HgCl₂ and CuCl₂ is also evident in the pH
533 impacts showing higher acidification after 24h than after 2h incubation (Fig. 2). The following
534 decrease in CO₂ after 3 months (down to ~145 μM) points to other processes. The precipitation of Hg
535 and Cu carbonates, given their high saturation index values (Tab. 2), would be consistent with the
536 decrease in CO₂ concentrations observed between three weeks and three months. Calcite precipitation
537 is typically observed in supersaturated solutions within 48h (Kim et al., 2020). Hence, it is realistic to

538 consider that Hg and Cu carbonate precipitation influenced the CO₂ concentration within the
539 preserved samples over the three months of storage time. Impacts of Hg or Cu carbonate precipitation
540 is not evident after three weeks likely because of slow but persistent CO₂ production in presence of
541 HgCl₂ and CuCl₂ related to acidification as described above (Fig. 1). However, after three weeks, this
542 production likely weakens and is counterbalanced by increasing carbonate precipitation.

543 Overall, the addition of HgCl₂ or CuCl₂ following sampling increased CO₂ concentrations by 47%
544 within the first 24h compared to the unfixed consistent with the -0.16 to -0.21 pH-unit acidification
545 observed over the same time in the pH incubation experiment (Fig. 2) and the pH estimated with
546 PHREEQC without the interaction with dissolved organic matter (Tab. 2). In fact, introducing pH and
547 CO₂ concentration values of 6.40–6.45 and 130 μM, respectively, for the samples preserved with
548 HgCl₂ and CuCl₂ into Eqs. 1 and 2 yields DIC concentrations (C_T) of about 270 μM at t=24h. These
549 DIC concentrations are almost equal to those calculated for the unfixed samples and those preserved
550 with AgNO₃ at t = 24h, i.e., with a pH of 6.73 and CO₂ concentration of 88 μM. Interestingly, the
551 concentration of CO₂ in the samples preserved with HgCl₂ and CuCl₂ continue to increase up to ~160
552 μM after 3 weeks. Given that oxic respiration is inhibited (Fig. 1), this additional CO₂ is believed to
553 originate from progressive release of protons following relatively slow complexation of Hg²⁺ with
554 dissolved organic matter (Khwaja et al., 2006; Miller et al., 2009; Skjellberg, 2008). Note that
555 PHREEQC could not predict complexation of Hg²⁺ with dissolved organic matter given that we
556 neglected the effect of dissolved organic matter.

557 Unlike the AgNO₃-fixed samples, all the other samples showed an initial increase in N₂O
558 concentration from 24h to 3 weeks, followed by a decrease from three weeks to 3 months. Similar
559 patterns of net N₂O production followed by net consumption were also reported in short-term
560 incubations of seawater from the high latitude Atlantic Ocean, although over much shorter timescales,
561 i.e., 48 and 96h (Rees et al., 2021). The large difference in kinetics between the latter experiment
562 (Rees et al., 2021) and our incubation might be attributable to differences in incubation temperature
563 where the seawater from the high latitude Atlantic Ocean was incubated at ambient temperatures
564 while our samples were kept at +4°C. Other difference in the experimental setup might have also
565 played a role. The lack of inhibition of N₂O production and consumption in the samples preserved
566 with HgCl₂ and CuCl₂ can be attributed to the fact that N₂O production tends to increase under
567 increasing acidic conditions (Knowles, 1982; Mørkved et al., 2007; Seitzinger, 1988). In fact, the
568 mole fraction of N₂O produced during denitrification increases compared to N₂ as pH decreases
569 (Knowles, 1982).

570



571

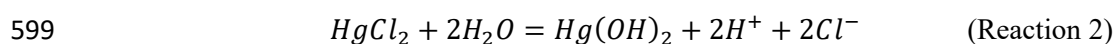
572 **Figure 4.** Comparison of observed (circles) and predicted (blue line) relative overestimation (E) of
 573 CO₂ concentrations caused by HgCl₂ fixation in Lake Lundebyvannet samples as a function of pH
 574 (top panel) or proton concentration (bottom panel). The black line shows the best fit of the regression
 575 analysis. White symbols represent samples for which the bicarbonate concentration in the unfixed
 576 samples ($[HCO_3^-]_i$) is nearly equal to CO₂ overestimation ($[CO_2]_{ex}$), i.e., $\pm 20\mu\text{M}$ (equivalent to a pH
 577 error of 0.05), while red and blue symbols represent samples for which initial bicarbonate
 578 concentration was lower and higher than the CO₂ overestimation, respectively.

579 4.3 Using PHREEQC to estimate acidification caused by HgCl₂ in samples from Lake Lundebyvannet

580 As for the samples from Lake Svartkulp as described above, the overestimation of CO₂ concentration
 581 in the samples from Lake Lundebyvannet fixed with HgCl₂ (161 μM added; Fig. 3) likely stems from
 582 the acidification shifting the carbonate equilibrium from bicarbonate to CO₂. In fact, PHREEQC
 583 predicted a decrease of 0.6 to 1.8 units of pH related to HgCl₂ addition in these samples (Fig. S1).

584 The relative overestimation of CO₂ (*E* in Fig. 4) followed a typical exponential increase reflecting the
 585 decrease in absolute CO₂ concentration with increasing pH (Stumm & Morgan, 1981) caused here by
 586 phytoplankton photosynthesis. In fact, the exponential increase in CO₂ overestimation is easily
 587 predicted by Eq. (9) with an equivalent level of accuracy as the optimized exponential function (Fig.
 588 4). Consistently, the relative overestimation of CO₂ (*E*) shows an inverse decrease with [H⁺] that is
 589 well reproduced by a simple inverse function ($3.25 \times 10^{-5}/[H^+]$; RMSE=44%, R²=0.81, p<0.0001;
 590 Fig. 4) and predicted by Eq. (15), with an α value of 1. Combining Eqs. 8 and 15 and solving it with
 591 pH values estimated from PHREEQC (Fig. S1) for α yields values ranging between 0.72 and 0.89
 592 with an average of 0.85. Unexpectedly, this average α value is almost equal to the ratio of the inverse
 593 function coefficient and K₁, i.e., $\frac{3.25 \times 10^{-5}}{K_1} = 0.87$. Hence, the relative overestimation of CO₂ (*E*)
 594 caused by HgCl₂ fixation is easily predicted by the change in bicarbonate equilibrium knowing the
 595 proton release from HgCl₂ addition, here estimated with PHREEQC.

596 Hence, PHREEQC can be used to predict decrease in pH caused by HgCl₂ fixation, if sufficient
 597 knowledge is gathered on the ionic water composition. Proton release during HgCl₂ fixation can be
 598 represented by the following reaction:



600 From reaction 2, it becomes evident that the initial concentration of chloride in the water samples will
 601 likely limit HgCl₂ dissociation and proton release. This is a likely mechanism occurring in seawater
 602 where HgCl₂ has been shown to cause a decrease in pH, although at a negligible level with a
 603 maximum decrease in pH of -0.01 (Chou et al., 2016).

604 Figure 3 shows that a range of water samples were associated with a relative CO₂ overestimation (*E*)
 605 that substantially deviated from the overestimation predicted with Eq. 12 (red and blue symbols in
 606 Fig. 4). In fact, some samples had a higher initial bicarbonate content ($[HCO_3^-]_i$) than the excess CO₂
 607 concentration ($[CO_2]_{ex}$), while other showed the opposite. The former case (blue symbols in Fig. 4)
 608 can easily be explained by a higher buffering capacity of the sampled water, i.e., a higher pH after
 609 HgCl₂-fixation than that predicted by PHREEQC related to a different water composition. Indeed, the
 610 concentration of major elements in the water from Lake Lundebyvannet may vary significantly over
 611 time, and in absence of data, we considered that the water composition, except for DIC, pH and

612 HgCl₂, was constant over time. By contrast, samples associated with $[CO_2]_{ex}$ being larger than
613 $[HCO_3^-]_i$ are more enigmatic. In order to shed light on possible explanations, we visually inspected
614 trends between empirical deviations from predictions, i.e., residuals, and *in situ* temperature or pH.
615 Absolute values of residuals showed a progressive increase with pH and *in situ* temperature which is
616 in agreement with decreasing precision of the headspace method with increasing temperature and pH
617 (Koschorreck et al., 2021). In fact, CO₂ is less soluble at higher temperature, hence more gas can
618 evade during sampling, and thus the error increases with *in situ* temperature. In addition, at higher pH,
619 CO₂ concentration decreases and consequently the absolute error on CO₂ quantification becomes
620 larger relative to measured CO₂ concentration. Interestingly, many of the high residual values were
621 not evenly distributed across the year, nor across the summer and were rather associated with only a
622 few specific sampling events during summer (Fig. S2). This suggests that degassing could have
623 occurred due to high ambient temperature in the field. Water associated with $[CO_2]_{ex}$ being larger
624 than $[HCO_3^-]_i$ (red symbols in Fig. 4 and S4) could have been subject to a larger degassing in the
625 samples collected for DIC analysis than the samples for GC analysis. On the other hand, degassing
626 was likely larger for samples for GC analysis than for DIC analysis for water associated with
627 $[HCO_3^-]_i$ being larger than $[CO_2]_{ex}$ (blue symbols in Fig. 4 and Fig. S2). In addition to degassing and
628 temperature effects, errors in pH measurements can also cause a large misestimation of CO₂
629 concentration from DIC analysis, and this error increases exponentially with pH following the shift in
630 carbonate equilibrium. In summary, our analysis is consistent with that of Koschorreck et al. (2021)
631 showing that errors in the determination of CO₂ concentrations are smaller at lower pH and lower
632 temperature (Fig. S2).

633 4.4. Implications for the estimation of lake and reservoir C cycling and recommendations

634 Using HgCl₂ or CuCl₂ to preserve dissolved gas samples in poorly buffered water samples has large
635 impacts on CO₂ concentrations with considerable risk of leading to incorrect interpretations. The risk
636 of mis-estimating CO₂ concentration due to HgCl₂ and CuCl₂ preservation is the highest when natural
637 water pH is close to the first carbonic acid dissociation constant ($pK_1 = 6.41$ at 25°C; Stumm &
638 Morgan, 1996). It implies that any small shift in pH will have a significant impact in the carbonate
639 equilibrium between bicarbonate to CO₂. The risk is also the highest in the lowest ionic strength
640 waters. In that respect, low-ionic strength, slightly acidic to neutral, moderately humic lakes
641 commonly found in Norway (de Wit et al., 2023), large parts of Sweden (Valina et al. 2014), and
642 Finland, Atlantic Canada (Houle et al., 2022), Ontario, Québec, and North-East USA (Skjelkvåle and
643 de Wit 2011; Weyhenmeyer et al., 2019) are the most prone to errors in CO₂ concentrations related to
644 HgCl₂ or CuCl₂ preservation. A significant part of these low-ionic strength lakes become increasingly
645 sensitive to changes in nutrients with strong impacts on their role in carbon cycling (Myrstener et al.,
646 2022). In this context, it is crucial to avoid mis-estimation of CO₂ concentrations and thus avoid use
647 of HgCl₂ or CuCl₂ to ensure a robust understanding of the role of autotrophic processes in lake C

648 cycling. Below we describe the implications for the lake C budget of Lundebyvannet as an example of
649 a mis-estimation of the role of photosynthesis in a typical productive boreal lake.

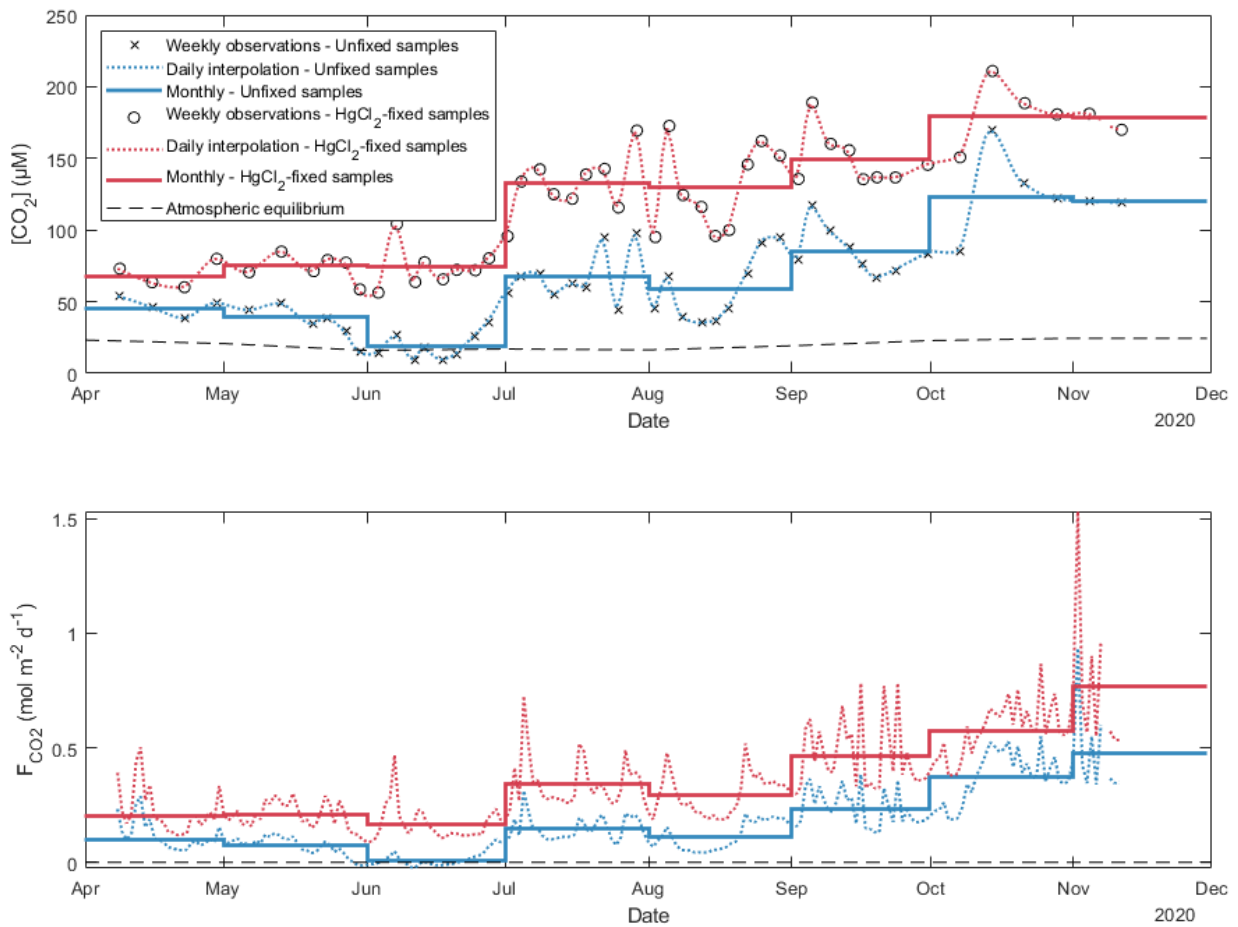
650 In Lake Lundebyvannet, over the ice-free season, average CO₂ concentrations determined following
651 HgCl₂-fixation and GC analysis were 82% higher than those obtained from DIC analyses (Tab. 3; Fig.
652 5 and S3). CO₂ concentrations obtained from HgCl₂-fixed samples created the illusion that Lake
653 Lundebyvannet was a steady net source of CO₂ to the atmosphere over the ice-free season with large
654 CO₂ saturation deficit (Fig. 3) while, in reality, the lake switched from being a net source in May, to a
655 net sink over a few weeks in June, and returning to a net source in July (Fig. 5 and S3). Indeed,
656 monthly CO₂ overestimation related to HgCl₂-fixation reached about 300% in June (Tab. 3).
657 Propagating this overestimation into the estimates of CO₂ diffusion fluxes with typical wind-based
658 models yields overestimation of CO₂ fluxes of 108–112% over the ice-free season and up to 2100% in
659 June (Tab. 3 and S3). Hence, interpreting CO₂ data without correcting for CO₂ overestimation caused
660 by HgCl₂-fixation leads to negligence of the role of photosynthesis in lake C cycling with major
661 implications for current and future predictions of lake CO₂ emissions.

662 The use of HgCl₂ to preserve water samples prior to dissolved gas analyses is part of the current
663 guidelines for greenhouse gas measurements in freshwater reservoirs (Machado Damazio et al., 2012;
664 UNESCO/IHA, 2008, 2010). Hence, there is a risk of overestimating CO₂ concentrations and
665 emissions, in absence of discrete measurement of emissions, from hydropower reservoirs with
666 consequence on the present and expected greenhouse gas footprint from hydroelectricity. To ensure
667 precise estimation of greenhouse concentration and, possibly, emission from hydropower, the use of
668 HgCl₂ should therefore be discontinued.

669 **5. Conclusion**

670 Mercury is a potent neurotoxin for humans and toxic for the environment and its use should be
671 discouraged, notably following the Minamata convention on mercury, a global treaty ratified by 126
672 countries (16 December 2020) to protect human health and the environment from the adverse effects
673 of mercury. This study further questions the use of HgCl₂ for preservation of poorly buffered (low
674 ionic strength) water samples with high DOC concentration for analysis of dissolved gases in the
675 laboratory. Although CuCl₂ is less toxic, it behaved similarly to HgCl₂ and cannot be recommend. In
676 fact, both chlorinated inhibitors caused a significant decrease in pH shifting the carbonate equilibrium
677 towards CO₂ and are also suspected to promote carbonate precipitation over long-term storage. The
678 only promising inhibitor tested in this study was AgNO₃ notably for dissolved CO₂, CH₄ and N₂O.
679 Silver nitrate is a suitable substitute for HgCl₂ in low-ionic strength waters, further tests should be
680 carried out with a range of inhibitor concentration and more diverse water samples. The use of
681 chemical inhibitors may not be the best approach. Alternatives exist, such as directly measuring gas
682 concentrations *in situ* with sensors, or sampling the headspace out in the field, and bringing back gas

683 samples (e.g., Cole et al., 1994; Karlsson et al., 2013; Kling et al., 1991; Valiente et al., 2022), rather
684 than water samples, to the lab for gas chromatography analyses. However, care must be taken to know
685 the exact equilibration temperature (Koschorreck et al., 2021) and to avoid gas exchange with the
686 atmosphere as well as to use a clean background gas during headspace equilibration which can be
687 challenging in remote environments under harsh meteorological conditions.



688

689 **Figure 5.** Daily and monthly surface CO₂ concentrations ([CO₂]; top panel) and diffusion fluxes
 690 (F_{CO₂}; bottom panel) at the water-atmosphere interface from Lake Lundebyvannet (also in Tab. 3).
 691 Unfixed samples were obtained by DIC analysis. Daily [CO₂] was interpolated from weekly data
 692 using a modified spline (see text for details). Diffusion fluxes were calculated following Cole &
 693 Caraco (1998).

694 We further advise against interpretation of CO₂ concentration data from low ionic strength, circum-
695 neutral water samples preserved with HgCl₂ or CuCl₂. The overestimation of CO₂ concentration
696 caused by HgCl₂ can mask the effect of photosynthesis on lake carbon balance, creating the illusion
697 that lakes are net CO₂ sources when they are net CO₂ sinks. Our analysis from Lake Lundebyvannet
698 shows that HgCl₂ fixation led to an overestimation of the CO₂ concentration by a factor of 1.8, on
699 average, but approaching a factor of 4 during the peak photosynthetic period. An even larger impact is
700 expected on CO₂ diffusive fluxes which were overestimated by a factor of 2 on average and up to a
701 factor of >20 during peak photosynthesis. Interpreting such data would have underestimated the
702 current and future role of aquatic photosynthesis.

703 **Data availability**

704 All data supporting this study will be made available on a permanent repository upon acceptance, e.g.,
705 Hydroshare.

706 **Author contribution**

707 JET, AK, and TR supervised and PD, KN and FC contributed to the study design. JET, KN and TR
708 carried out the experiments. PD and TR performed the chemical analyses. JET and FC wrote the first
709 draft. FC performed the modelling, data, and statistical analyses, and drafted the figures. All co-
710 authors edited the manuscript.

711 **Competing interests**

712 The contact author has declared that none of the authors has any competing interests.

713 **Acknowledgements**

714 We are grateful to Benoît Demars for research assistance, coordination, and useful comments and
715 discussions on an earlier version of this manuscript and to Heleen de Wit for discussions. Research
716 was funded by NIVA and through the Global Change at Northern Latitude (NoLa) project #200033.

717

718 **References**

- 719 Akima, H. (1974). A method of bivariate interpolation and smooth surface fitting based on local
720 procedures. *Communications of the ACM*, 17(1), 18–20.
721 <https://doi.org/10.1145/360767.360779>
- 722 Allison, J., Brown, D., & Novo-Gradac, K. (1991). *MINTEQA2/PRODEFA2, a geochemical*
723 *assessment model for environmental systems: Version 3. 0 user's manual*. GA: US
724 Environmental Protection Agency.
- 725 Amorim, M. J. B., & Scott-Fordsmand, J. J. (2012). Toxicity of copper nanoparticles and CuCl₂ salt
726 to *Enchytraeus albidus* worms: Survival, reproduction and avoidance responses.
727 *Environmental Pollution*, 164, 164–168. <https://doi.org/10.1016/j.envpol.2012.01.015>

- 728 Borges, A. V., Darchambeau, F., Lambert, T., Morana, C., Allen, G. H., Tambwe, E., Toengaho
729 Sembaito, A., Mambo, T., Nlandu Wabakhangazi, J., Descy, J.-P., Teodoru, C. R., &
730 Bouillon, S. (2019). Variations in dissolved greenhouse gases (CO₂, CH₄, N₂O) in the Congo
731 River network overwhelmingly driven by fluvial-wetland connectivity. *Biogeosciences*,
732 *16*(19), 3801–3834. <https://doi.org/10.5194/bg-16-3801-2019>
- 733 Carroll J.J., Slupsky J.D. & Mather A.E. (1991) The solubility of carbon dioxide in water at low
734 pressure. *Journal of Physical and Chemical Reference Data*, **20**, 1201-1209.
735 <https://doi.org/10.1063/1.555900>
- 736 Chen, C. Y., Driscoll, C., Eagles-Smith, C. A., Eckley, C. S., Gay, D. A., Hsu-Kim, H., Keane, S. E.,
737 Kirk, J. L., Mason, R. P., Obrist, D., Selin, H., Selin, N. E., & Thompson, M. R. (2018). A
738 Critical Time for Mercury Science to Inform Global Policy. *Environmental Science &*
739 *Technology*, *52*(17), 9556–9561. <https://doi.org/10.1021/acs.est.8b02286>
- 740 Chen H., Johnston R.C., Mann B.F., Chu R.K., Tolic N., Parks J.M. & Gu B. (2017) Identification of
741 mercury and dissolved organic matter complexes using ultrahigh resolution mass
742 spectrometry. *Environmental Science & Technology Letters*, **4**, 59-65.
743 <https://doi.org/10.1021/acs.estlett.6b00460>
- 744 Chou W.C., Gong G.C., Yang C.Y. & Chuang K.Y. (2016) A comparison between field and
745 laboratory pH measurements for seawater on the East China Sea shelf. *Limnology and*
746 *Oceanography-Methods*, **14**, 315-322. <https://doi.org/10.1002/lom3.10091>
- 747 Ciavatta L. & Grimaldi M. (1968) The hydrolysis of mercury(II) chloride, HgCl₂. *Journal of*
748 *Inorganic and Nuclear Chemistry*, **30**, 563-581. [https://doi.org/10.1016/0022-1902\(68\)80483-](https://doi.org/10.1016/0022-1902(68)80483-X)
749 X
- 750 Clayer, F., Thrane, J.-E., Brandt, U., Dörsch, P., & de Wit, H. A. (2021). Boreal Headwater
751 Catchment as Hot Spot of Carbon Processing From Headwater to Fjord. *Journal of*
752 *Geophysical Research: Biogeosciences*, *126*(12), e2021JG006359.
753 <https://doi.org/10.1029/2021JG006359>
- 754 Cole, J. J., Caraco, N. F., Kling, G. W., & Kratz, T. K. (1994). Carbon Dioxide Supersaturation in the
755 Surface Waters of Lakes. *Science*, *265*(5178), Article 5178.
756 <https://doi.org/10.1126/science.265.5178.1568>
- 757 Cole, J. J., & Caraco, N. F. (1998). Atmospheric exchange of carbon dioxide in a low-wind
758 oligotrophic lake measured by the addition of SF₆. *Limnology and Oceanography*, *43*(4),
759 Article 4. <https://doi.org/10.4319/lo.1998.43.4.0647>
- 760 Crusius, J., & Wanninkhof, R. (2003). Gas transfer velocities measured at low wind speed over a lake.
761 *Limnology and Oceanography*, *48*(3), Article 3. <https://doi.org/10.4319/lo.2003.48.3.1010>
- 762 Deheyn, D. D., Bencheikh-Latmani, R., & Latz, M. I. (2004). Chemical speciation and toxicity of
763 metals assessed by three bioluminescence-based assays using marine organisms.
764 *Environmental Toxicology*, *19*(3), 161–178. <https://doi.org/10.1002/tox.20009>
- 765 de Wit, H. A., Garmo, Ø. A., Jackson-Blake, L. A., Clayer, F., Vogt, R. D., Austnes, K., Kaste, Ø.,
766 Gundersen, C. B., Guerrero, J. L., & Hindar, A. (2023). Changing Water Chemistry in One
767 Thousand Norwegian Lakes During Three Decades of Cleaner Air and Climate Change.
768 *Global Biogeochemical Cycles*, *37*(2), e2022GB007509.
769 <https://doi.org/10.1029/2022GB007509>
- 770 Dickson A.G., Sabine C.L. & Christian J.R. (2007) *Guide to best practices for ocean CO₂*
771 *measurements*, North Pacific Marine Science Organization.
- 772 Duan, Z., & Mao, S. (2006). A thermodynamic model for calculating methane solubility, density and
773 gas phase composition of methane-bearing aqueous fluids from 273 to 523K and from 1 to
774 2000bar. *Geochimica et Cosmochimica Acta*, *70*(13), Article 13.
775 <https://doi.org/10.1016/j.gca.2006.03.018>
- 776 Foti C., Giuffrè O., Lando G. & Sammartano S. (2009) Interaction of inorganic mercury (II) with
777 polyamines, polycarboxylates, and amino acids. *Journal of Chemical & Engineering Data*,
778 **54**, 893-903. <https://doi.org/10.1021/jc800685c>
- 779 *Frost API*. (2022). <https://frost.met.no/index.html>
- 780 Guérin, F., Abril, G., Richard, S., Burban, B., Reynouard, C., Seyler, P., & Delmas, R. (2006).
781 Methane and carbon dioxide emissions from tropical reservoirs: Significance of downstream
782 rivers. *Geophysical Research Letters*, *33*(21). <https://doi.org/10.1029/2006GL027929>

- 783 Guérin, F., Abril, G., Serça, D., Delon, C., Richard, S., Delmas, R., Tremblay, A., & Varfalvy, L.
784 (2007). Gas transfer velocities of CO₂ and CH₄ in a tropical reservoir and its river
785 downstream. *Journal of Marine Systems*, 66(1), Article 1.
786 <https://doi.org/10.1016/j.jmarsys.2006.03.019>
- 787 Halmi, M. I. E., Kassim, A., & Shukor, M. Y. (2019). Assessment of heavy metal toxicity using a
788 luminescent bacterial test based on *Photobacterium* sp. Strain MIE. *Rendiconti Lincei. Scienze*
789 *Fisiche e Naturali*, 30(3), 589–601. <https://doi.org/10.1007/s12210-019-00809-5>
- 790 Hagman, C. H. C., Ballot, A., Hjermann, D. Ø., Skjelbred, B., Brettum, P., & Ptacnik, R. (2015). The
791 occurrence and spread of *Gonyostomum semen* (Ehr.) Diesing (Raphidophyceae) in
792 Norwegian lakes. *Hydrobiologia*, 744(1), 1–14. <https://doi.org/10.1007/s10750-014-2050-y>
- 793 Hamme R.C. & Emerson S.R. (2004) The solubility of neon, nitrogen and argon in distilled water and
794 seawater. *Deep-Sea Research Part I-Oceanographic Research Papers*, 51, 1517-1528.
795 <https://doi.org/10.1016/j.dsr.2004.06.009>
- 796 Hassen A., Saidi N., Cherif M. & Boudabous A. (1998) Resistance of environmental bacteria to heavy
797 metals. *Bioresource technology*, 64, 7-15. [https://doi.org/10.1016/S0960-8524\(97\)00161-2](https://doi.org/10.1016/S0960-8524(97)00161-2)
- 798 Hessen, D. O., Håll, J. P., Thrane, J.-E., & Andersen, T. (2017). Coupling dissolved organic carbon,
799 CO₂ and productivity in boreal lakes. *Freshwater Biology*, 62(5), 945–953.
800 <https://doi.org/10.1111/fw.12914>
- 801 Hilgert, S., Scapulatempo Fernandes, C. V., & Fuchs, S. (2019). Redistribution of methane emission
802 hot spots under drawdown conditions. *Science of The Total Environment*, 646, 958–971.
803 <https://doi.org/10.1016/j.scitotenv.2018.07.338>
- 804 Horvatić J. & Peršić V. (2007) The effect of Ni²⁺, Co²⁺, Zn²⁺, Cd²⁺ and Hg²⁺ on the growth
805 rate of marine diatom *Phaeodactylum tricornutum* Bohlin: microplate growth inhibition test.
806 *Bulletin of Environmental Contamination and Toxicology*, 79, 494-498.
807 <https://doi.org/10.1007/s00128-007-9291-7>
- 808 Houle, D., Augustin, F., & Couture, S. (2022). Rapid improvement of lake acid–base status in
809 Atlantic Canada following steep decline in precipitation acidity. *Canadian Journal of*
810 *Fisheries and Aquatic Sciences*, 79(12), 2126–2137. <https://doi.org/10.1139/cjfas-2021-0349>
- 811 IEA. (2020). *Key World Energy Statistics 2020*. IEA, International Energy Agency.
812 <https://www.iea.org/reports/key-world-energy-statistics-2020>
- 813 Karlsson, J., Giesler, R., Persson, J., & Lundin, E. (2013). High emission of carbon dioxide and
814 methane during ice thaw in high latitude lakes. *Geophysical Research Letters*, 40(6), Article
815 6. <https://doi.org/10.1002/grl.50152>
- 816 Khwaja, A. R., Bloom, P. R., & Brezonik, P. L. (2006). Binding Constants of Divalent Mercury
817 (Hg²⁺) in Soil Humic Acids and Soil Organic Matter. *Environmental Science & Technology*,
818 40(3), 844–849. <https://doi.org/10.1021/es051085c>
- 819 Kim, D., Mahabadi, N., Jang, J., & van Paassen, L. A. (2020). Assessing the Kinetics and Pore-Scale
820 Characteristics of Biological Calcium Carbonate Precipitation in Porous Media using a
821 Microfluidic Chip Experiment. *Water Resources Research*, 56(2), e2019WR025420.
822 <https://doi.org/10.1029/2019WR025420>
- 823 Kling, G. W., Kipphut, G. W., & Miller, M. C. (1991). Arctic Lakes and Streams as Gas Conduits to
824 the Atmosphere: Implications for Tundra Carbon Budgets. *Science*, 251(4991), 298–301.
825 <https://doi.org/10.1126/science.251.4991.298>
- 826 Knowles, R. (1982). Denitrification. *Microbiological Reviews*, 46(1), 43–70.
827 <https://doi.org/10.1128/mr.46.1.43-70.1982>
- 828 Kokic, J., Wallin, M. B., Chmiel, H. E., Denfeld, B. A., & Sobek, S. (2015). Carbon dioxide evasion
829 from headwater systems strongly contributes to the total export of carbon from a small boreal
830 lake catchment. *Journal of Geophysical Research: Biogeosciences*, 120(1), 13–28.
831 <https://doi.org/10.1002/2014JG002706>
- 832 Koschorreck, M., Prairie, Y. T., Kim, J., & Marcé, R. (2021). Technical note: CO₂ is not like CH₄ –
833 limits of and corrections to the headspace method to analyse *p*CO₂ in fresh water.
834 *Biogeosciences*, 18(5), 1619–1627. <https://doi.org/10.5194/bg-18-1619-2021>
- 835 Larrañaga, M., Lewis, R., & Lewis, R. (2016). *Hawley's Condensed Chemical Dictionary*, Sixteenth
836 Edition. i–xiii. <https://doi.org/10.1002/9781119312468.fmatter>

- 837 Liang X., Lu X., Zhao J., Liang L., Zeng E.Y. & Gu B. (2019) Stepwise reduction approach reveals
838 mercury competitive binding and exchange reactions within natural organic matter and mixed
839 organic ligands. *Environmental Science & Technology*, **53**, 10685-10694.
840 <https://doi.org/10.1021/acs.est.9b02586>
- 841 Machado Damazio, J., Cordeiro Geber de Melo, A., Piñeiro Maceira, M. E., Medeiros, A., Negrini,
842 M., Alm, J., Schei, T. A., Tateda, Y., Smith, B., & Nielsen, N. (2012). *Guidelines for*
843 *quantitative analysis of net GHG emissions from reservoirs: Volume 1: Measurement*
844 *Programmes and Data Analysis*. International Energy Agency (IEA).
845 https://www.ieahydro.org/media/992f6848/GHG_Guidelines_22October2012_Final.pdf
- 846 Magen, C., Lapham, L. L., Pohlman, J. W., Marshall, K., Bosman, S., Casso, M., & Chanton, J. P.
847 (2014). A simple headspace equilibration method for measuring dissolved methane.
848 *Limnology and Oceanography: Methods*, **12**(9), 637–650.
849 <https://doi.org/10.4319/lom.2014.12.637>
- 850 Miller, C. L., Southworth, G., Brooks, S., Liang, L., & Gu, B. (2009). Kinetic Controls on the
851 Complexation between Mercury and Dissolved Organic Matter in a Contaminated
852 Environment. *Environmental Science & Technology*, **43**(22), 8548–8553.
853 <https://doi.org/10.1021/es901891t>
- 854 Millero F.J., Huang F. & Laferiere A.L. (2002) Solubility of oxygen in the major sea salts as a
855 function of concentration and temperature. *Marine Chemistry*, **78**, 217-230.
856 [https://doi.org/10.1016/S0304-4203\(02\)00034-8](https://doi.org/10.1016/S0304-4203(02)00034-8)
- 857 Myrstener, M., Fork, M. L., Bergström, A.-K., Puts, I. C., Hauptmann, D., Isles, P. D. F., Burrows, R.
858 M., & Sponseller, R. A. (2022). Resolving the Drivers of Algal Nutrient Limitation from
859 Boreal to Arctic Lakes and Streams. *Ecosystems*, **25**(8), 1682–1699.
860 <https://doi.org/10.1007/s10021-022-00759-4>
- 861 Mørkved, P. T., Dörsch, P., & Bakken, L. R. (2007). The N₂O product ratio of nitrification and its
862 dependence on long-term changes in soil pH. *Soil Biology and Biochemistry*, **39**(8), 2048–
863 2057. <https://doi.org/10.1016/j.soilbio.2007.03.006>
- 864 NILU. (2022). *EBAS*. <https://ebas-data.nilu.no/Default.aspx>
- 865 Nowack, B., Krug, H. F., & Height, M. (2011). 120 Years of Nanosilver History: Implications for
866 Policy Makers. *Environmental Science & Technology*, **45**(4), 1177–1183.
867 <https://doi.org/10.1021/es103316q>
- 868 NPIRS. (2023). *Purdue University*. <https://www.npirs.org/public>
- 869 Okuku, E. O., Bouillon, S., Tole, M., & Borges, A. V. (2019). Diffusive emissions of methane and
870 nitrous oxide from a cascade of tropical hydropower reservoirs in Kenya. *Lakes &*
871 *Reservoirs: Science, Policy and Management for Sustainable Use*, **24**(2), 127–135.
872 <https://doi.org/10.1111/lre.12264>
- 873 Parkhurst, D. L., & Appelo, C. A. J. (2013). *Description of input and examples for PHREEQC version*
874 *3—A computer program for speciation, batch-reaction, one-dimensional transport, and*
875 *inverse geochemical calculations: U.S. Geological Survey Techniques and Methods* (book 6,
876 chap. A43; p. 497). USGS. <http://pubs.usgs.gov/tm/06/a43/>
- 877 Powell K.J., Brown P.L., Byrne R.H., Gajda T., Hefter G., Sjöberg S. & Wanner H. (2004) Chemical
878 speciation of Hg (II) with environmental inorganic ligands. *Australian Journal of Chemistry*,
879 **57**, 993-1000. <https://doi.org/10.1071/CH04063>
- 880 Rai L.C., Gaur J.P. & Kumar H.D. (1981) Phycology and heavy-metal pollution. *Biological Reviews*,
881 **56**, 99-151. <https://doi.org/10.1111/j.1469-185X.1981.tb00345.x>
- 882 Ratte, H. T. (1999). Bioaccumulation and toxicity of silver compounds: A review. *Environmental*
883 *Toxicology and Chemistry*, **18**(1), 89–108. <https://doi.org/10.1002/etc.5620180112>
- 884 Rees, A. P., Brown, I. J., Jayakumar, A., Lessin, G., Somerfield, P. J., & Ward, B. B. (2021).
885 Biological nitrous oxide consumption in oxygenated waters of the high latitude Atlantic
886 Ocean. *Communications Earth & Environment*, **2**(1), Article 1.
887 <https://doi.org/10.1038/s43247-021-00104-y>
- 888 Rippner, D. A., Margenot, A. J., Fakra, S. C., Aguilera, L. A., Li, C., Sohng, J., Dynarski, K. A.,
889 Waterhouse, H., McElroy, N., Wade, J., Hind, S. R., Green, P. G., Peak, D., McElrone, A. J.,
890 Chen, N., Feng, R., Scow, K. M., & Parikh, S. J. (2021). Microbial response to copper oxide

- 891 nanoparticles in soils is controlled by land use rather than copper fate. *Environmental*
 892 *Science: Nano*, 8(12), 3560–3576. <https://doi.org/10.1039/D1EN00656H>
- 893 Rohrlack T., Frostad P., Riise G. & Hagman C.H.C. (2020) Motile phytoplankton species such as
 894 *Gonyostomum* semen can significantly reduce CO₂ emissions from boreal lakes.
 895 *Limnologica*, **84**, 125810. <https://doi.org/10.1016/j.limno.2020.125810>
- 896 Schubert, C. J., Diem, T., & Eugster, W. (2012). Methane Emissions from a Small Wind Shielded
 897 Lake Determined by Eddy Covariance, Flux Chambers, Anchored Funnels, and Boundary
 898 Model Calculations: A Comparison. *Environmental Science & Technology*, 46(8), 4515–
 899 4522. <https://doi.org/10.1021/es203465x>
- 900 Seitzinger, S. P. (1988). Denitrification in freshwater and coastal marine ecosystems: Ecological and
 901 geochemical significance. *Limnology and Oceanography*, 33(4part2), 702–724.
 902 <https://doi.org/10.4319/lo.1988.33.4part2.0702>
- 903 Silver S. & Phung L.T. (2005) A bacterial view of the periodic table: genes and proteins for toxic
 904 inorganic ions. *Journal of Industrial Microbiology & Biotechnology*, **32**, 587-605.
 905 <https://doi.org/10.1007/s10295-005-0019-6>
- 906 Skjelkvåle, B. L., & de Wit, H. A. (2011). Trends in precipitation chemistry, surface water chemistry
 907 and aquatic biota in acidified areas in Europe and North America from 1990 to 2008 (ICP
 908 Waters report 106/2011). In 126. Norsk institutt for vannforskning.
 909 <https://niva.brage.unit.no/niva-xmlui/handle/11250/215591>
- 910 Skyllberg, U. (2008). Competition among thiols and inorganic sulfides and polysulfides for Hg and
 911 MeHg in wetland soils and sediments under suboxic conditions: Illumination of controversies
 912 and implications for MeHg net production. *Journal of Geophysical Research:*
 913 *Biogeosciences*, 113(G2). <https://doi.org/10.1029/2008JG000745>
- 914 Sobek, S., Algesten, G., Bergström, A.-K., Jansson, M., & Tranvik, L. J. (2003). The catchment and
 915 climate regulation of pCO₂ in boreal lakes. *Global Change Biology*, 9(4), 630–641.
 916 <https://doi.org/10.1046/j.1365-2486.2003.00619.x>
- 917 Stumm W. & Morgan J.J. (1981) *Aquatic Chemistry. An introduction emphasizing chemical*
 918 *equilibria in natural waters*, Wiley Interscience, New York.
- 919 Stumm, W., & Morgan, J. J. (1996). *Aquatic chemistry: Chemical equilibria and rates in natural*
 920 *waters* (3rd ed.). Wiley.
- 921 Taipale S.J. & Sonninen E. (2009) The influence of preservation method and time on the delta C-13
 922 value of dissolved inorganic carbon in water samples. *Rapid Communications in Mass*
 923 *Spectrometry*, **23**, 2507-2510. <https://doi.org/10.1002/rcm.4072>
- 924 Takahashi H.A., Handa H., Sugiyama A., Matsushita M., Kondo M., Kimura H. & Tsujimura M.
 925 (2019) Filtration and exposure to benzalkonium chloride or sodium chloride to preserve water
 926 samples for dissolved inorganic carbon analysis. *Geochemical Journal*, **53**, 305-318.
 927 <https://doi.org/10.2343/geochemj.2.0570>
- 928 Thottathil, S. D., Reis, P. C. J., & Prairie, Y. T. (2019). Methane oxidation kinetics in northern
 929 freshwater lakes. *Biogeochemistry*, 143(1), Article 1. <https://doi.org/10.1007/s10533-019-00552-x>
- 930
- 931 Tipping E. (2007) Modelling the interactions of Hg(II) and methylmercury with humic substances
 932 using WHAM/Model VI. *Applied Geochemistry*, **22**, 1624-1635.
- 933 Tørseth, K., Aas, W., Breivik, K., Fjæraa, A. M., Fiebig, M., Hjellbrekke, A. G., Lund Myhre, C.,
 934 Solberg, S., & Yttri, K. E. (2012). Introduction to the European Monitoring and Evaluation
 935 Programme (EMEP) and observed atmospheric composition change during
 936 1972–2009. *Atmospheric Chemistry and Physics*, 12(12), 5447–5481.
 937 <https://doi.org/10.5194/acp-12-5447-2012>
- 938 Ullmann, F., Gerhartz, W., Yamamoto, Y. S., Campbell, F. T., Pfefferkorn, R., & Rounsaville, J. F.
 939 (1985). Ullmann's encyclopedia of industrial chemistry (5th, completely rev. ed ed.). VCH.
- 940 UNESCO/IHA. (2008). *Assessment of the GHG status of freshwater reservoirs: Scoping paper*
 941 *(IHP/GHG-WG/3; p. 28)*. UNESCO/IHA, International Hydropower Association -
 942 International Hydrological Programme, Working Group on Greenhouse Gas Status of
 943 Freshwater Reservoirs. <https://unesdoc.unesco.org/ark:/48223/pf0000181713>
- 944 UNESCO/IHA. (2010). *GHG Measurement Guidelines for Freshwater Reservoirs* (p. 154).
 945 UNESCO/IHA, International Hydropower Association.

- 946 [https://www.hydropower.org/publications/ghg-measurement-guidelines-for-freshwater-](https://www.hydropower.org/publications/ghg-measurement-guidelines-for-freshwater-reservoirs)
947 [reservoirs](https://www.hydropower.org/publications/ghg-measurement-guidelines-for-freshwater-reservoirs)
- 948 Vachon, D., & Prairie, Y. T. (2013). The ecosystem size and shape dependence of gas transfer
949 velocity versus wind speed relationships in lakes. *Canadian Journal of Fisheries and Aquatic*
950 *Sciences*, 70(12), Article 12. <https://doi.org/10.1139/cjfas-2013-0241>
- 951 Valiente, N., Eiler, A., Allesson, L., Andersen, T., Clayer, F., Crapart, C., Dörsch, P., Fontaine, L.,
952 Heuschele, J., Vogt, R., Wei, J., de Wit, H. A., & Hessen, D. O. (2022). *Catchment properties*
953 *as predictors of greenhouse gas concentrations across a gradient of boreal lakes.*
954 *10(880619)*. <https://doi.org/10.3389/fenvs.2022.880619>
- 955 Valinia, S., Englund, G., Moldan, F., Futter, M. N., Köhler, S. J., Bishop, K., & Fölster, J. (2014).
956 Assessing anthropogenic impact on boreal lakes with historical fish species distribution data
957 and hydrogeochemical modeling. *Global Change Biology*, 20(9), 2752–2764.
958 <https://doi.org/10.1111/gcb.12527>
- 959 van Grinsven, S., Oswald, K., Wehrli, B., Jegge, C., Zopfi, J., Lehmann, M. F., & Schubert, C. J.
960 (2021). Methane oxidation in the waters of a humic-rich boreal lake stimulated by
961 photosynthesis, nitrite, Fe(III) and humics. *Biogeosciences*, 18(10), 3087–3101.
962 <https://doi.org/10.5194/bg-18-3087-2021>
- 963 Wanninkhof, R. (2014). Relationship between wind speed and gas exchange over the ocean revisited.
964 *Limnology and Oceanography: Methods*, 12(6), Article 6.
965 <https://doi.org/10.4319/lom.2014.12.351>
- 966 Weiss R.F. & Price B.A. (1980) Nitrous oxide solubility in water and seawater. *Marine Chemistry*, 8,
967 347-359. [https://doi.org/10.1016/0304-4203\(80\)90024-9](https://doi.org/10.1016/0304-4203(80)90024-9)
- 968 Weyhenmeyer, G. A., Hartmann, J., Hessen, D. O., Kopáček, J., Hejzlar, J., Jacquet, S., Hamilton, S.
969 K., Verburg, P., Leach, T. H., Schmid, M., Flaim, G., Nöges, T., Nöges, P., Wentzky, V. C.,
970 Rogora, M., Rusak, J. A., Kosten, S., Paterson, A. M., Teubner, K., ... Zechmeister, T.
971 (2019). Widespread diminishing anthropogenic effects on calcium in freshwaters. *Scientific*
972 *Reports*, 9(1), Article 1. <https://doi.org/10.1038/s41598-019-46838-w>
- 973 Wilhelm E., Battino R. & Wilcock R.J. (1977) Low-pressure solubility of gases in liquid water.
974 *Chemical Reviews*, 77, 219-262. <https://doi.org/10.1021/cr60306a003>
- 975 Wilson J., Munizzi J. & Erhardt A.M. (2020) Preservation methods for the isotopic composition of
976 dissolved carbon species in non-ideal conditions. *Rapid Communications in Mass*
977 *Spectrometry*, 34. <https://doi.org/10.1002/rcm.8903>
- 978 Xiao, S., Yang, H., Liu, D., Zhang, C., Lei, D., Wang, Y., Peng, F., Li, Y., Wang, C., Li, X., Wu, G.,
979 & Liu, L. (2014). Gas transfer velocities of methane and carbon dioxide in a subtropical
980 shallow pond. *Tellus B: Chemical and Physical Meteorology*, 66(1), 23795.
981 <https://doi.org/10.3402/tellusb.v66.23795>
- 982 Xu F.F. & Imlay J.A. (2012) Silver(I), Mercury(II), Cadmium(II), and Zinc(II) Target Exposed
983 Enzymic Iron-Sulfur Clusters when They Toxicify Escherichia coli. *Applied and Environmental*
984 *Microbiology*, 78, 3614-3621. <https://doi.org/10.1128/aem.07368-11>
- 985 Yamamoto S., Alcauskas J.B. & Crozier T.E. (1976) Solubility of methane in distilled water and
986 seawater. *Journal of Chemical and Engineering Data*, 21, 78-80.
987 <https://doi.org/10.1021/je60068a029>
- 988 Yan, F., Sillanpää, M., Kang, S., Aho, K. S., Qu, B., Wei, D., Li, X., Li, C., & Raymond, P. A.
989 (2018). Lakes on the Tibetan Plateau as Conduits of Greenhouse Gases to the Atmosphere.
990 *Journal of Geophysical Research: Biogeosciences*, 123(7), 2091–2103.
991 <https://doi.org/10.1029/2017JG004379>
- 992 Yang H., Andersen T., Dorsch P., Tominaga K., Thrane J.E. & Hessen D.O. (2015) Greenhouse gas
993 metabolism in Nordic boreal lakes. *Biogeochemistry*, 126, 211-225.
994 <https://doi.org/10.1007/s10533-015-0154-8>

995